Investigations on Pulsed Electrochemical Finishing of Additively Manufactured Parts

M.Tech. Thesis

by

Sumantra Aarya
(2102103012)

Discipline of Mechanical Engineering

Indian Institute of Technology Indore

May 2023

Investigations on Pulsed Electrochemical Finishing of Additively Manufactured Parts

A Thesis

Submitted in partial fulfillment of the requirements for the award of the degree of

Master of Technology

in

Mechanical Engineering

With specialization in

Production and Industrial Engineering

by

Sumantra Aarya

Discipline of Mechanical Engineering

Indian Institute of Technology Indore

May 2023

Indian Institute of Technology Indore

Candidate's Declaration

I hereby certify that the work which is being presented in the thesis entitled **"Investigations on Pulsed Electrochemical Finishing of Additively Manufactured Parts"** in the partial fulfillment of the requirements for the award of the degree of **Master of Technology** in **Mechanical Engineering** with specialization in **Production and Industrial Engineering** and submitted in the **Department of Mechanical Engineering, Indian Institute of Technology Indore**, is an authentic record of my own work carried out during the time period from **May 2022 to May 2023** under the supervision of **Prof. Neelesh Kumar Jain** of Department of Mechanical Engineering.

The matter presented in this thesis has not been submitted by me for the award of any degree from any other institute.

Sumantra Aarya

Sumantra Aarya

This is to certify that the above statement made by the candidate is correct to the best of our knowledge.

30/05/2023

(Prof. Neelesh Kumar Jain)

Sumantra Aarya has successfully completed his M.Tech Oral Examination held on 26th May 2023

Harshvardhan Yadav

Signature of M.Tech Thesis Supervisors
Date:

Signature of Convener, DPGC
Date:

M. Jayaprakash 30.05.2023

Name and signature of PSPC member 1 with date: **Dr. Jayaprakash Murugesan (MEMS)**

Abhijit Ghosh 30/05/23

Name and signature of PSPC member 2 with date: **Dr. Abhijit Ghosh (MEMS)**

30/5/2023

Name and signature of PSPC member 3 with date: **Dr. Ashish Rajak (ME)**

31/05/2023

Signature of Head of Department with date:
(Acting)

ACKNOWLEDGEMENTS

I take this opportunity to express my deep sense of respect and gratitude towards **Prof. Neelesh Kumar Jain** for believing in me to carry out this work under their supervision. Their constant encouragement and constructive support have enabled this work to achieve its present from. Their innovative perspective towards things and his continuous pursuit for perfection has had a profound effect on me and has transformed me majorly. I feel great privileged to be one of their students.

My gratitude is also extended to my PSPC members **Dr. Jayaprakash Murugesan, Dr. Abhijit Ghosh and Dr. Ashish Rajak** for their guidance and cooperation. I express my deep sense of gratitude to PhD scholars Vivek Rana, Pradyumn Kumar Arya Bhavesh Choudhary and Pankaj Kumar for bearing with me, for supporting me morally and technically and always maintaining a homely atmosphere in the lab. Special thanks are extended to my colleagues Atluri Bharath Kumar, Bhavesh Jain, Akash Yadav, Ankit Gangwar and Rajat Verma for their help and suggestions whenever I needed them and for always giving me company. I am also thankful to Lab staff of Mechanical Engineering Labs and Central Workshop specially Mr. Anand C. Petare ASW, IIT Indore, Mr. Santosh Sharma and Mr. Sandeep Gour, Mr. Deepak Rathore, Mr. Vinay Mishra, Mr. Pawan Chouhan, Mr. Satish Kaushal, Mr. Rishi Raj for their cooperation.

Sumantra Aarya

Dedicated

to

My Parents

Abstract

Additively manufactured (AMed) parts have poor surface finish (average surface roughness 'Ra' value lying in a range from 10 to 20 μm), high porosity, and residual stresses which affect their properties, performance, service life, and reliability. Very high surface roughness values of AMed parts reduce their dimensional and geometrical accuracy and tolerances, increase stress concentration, wear, and friction, and fasten initiation and propagation of cracks thus making them unsuitable for many engineering applications. This necessitates reducing the surface roughness of AMed parts through surface finishing methods to make them usable for commercial engineering applications. Pulsed electrochemical finishing (PECF) is a non-contact type finishing process in which material is removed in a very controlled manner from the anodic workpiece at the atomic/molecule level according to Faraday's laws of electrolysis. If optimum values of its parameters and properly finished cathodic tool are used then PECF process has capability to reduce the surface roughness of AMed parts having simple as well as complex geometries. Therefore, the proposed research is aimed to achieve 'Ra' value of AMed parts less than 1 μm by PECF process. Different process parameters of PECF process such as finishing duration, composition and flow rate of electrolyte, pulse-on time, pulse-off time, voltage, and concentration were studied to identify their optimum value to have maximum reduction in surface roughness. It identified optimum values of 20 minutes as finishing duration, 75% NaCl and 25% $NaNO_3$ as electrolyte composition, 10 litre/minute as flow rate of electrolyte, 3 ms as pulse-on time, 6 ms as pulse-off time, 25 V as voltage and 15% as electrolyte concentration respectively. Results showed that AMed parts having percentage improvement rates in Ra and Ry as 59% and 68.7%, respectively employing the optimum values of PECF process parameters.

CONTENTS

List of Figures

List of Tables

Nomenclature

I	Amount of current passed in the IEG (A)
J	Current density in the IEG (A/mm2)
Ra	Arithmetical *Average* Roughness (μm)
Ry	Average Maximum Height (μm)
t	Finishing Duration (minutes)
V	Applied Voltage (volts)
C	Composition of electrolyte (%)
$Conc.$	Concentration of electrolyte (%)
F	Flow rate of electrolyte (l/min)
V_{PECF}	Volumetric material removal rate in PECF (mm3/s)
IEG	Inter-electrode gap (mm)
T_{on}	Pulse on time (ms)
T_{off}	Pulse off time (ms)
$PIRa$	Percentage Improvement in Arithmetical Average Roughness
$PIRy$	Percentage Improvement in Average Maximum Height

Abbreviations

AMP	Advanced Machining Processes
CNC	Computer Numeral Control
WEDM	Wire Electric Discharge Machining
DC	Direct Current
DOE	Design of Experiments
ECD	Electrochemical Dissolution
ECM	Electrochemical Machining
ECF	Electrochemical Finishing
IEG	Inter Electrode Gap
MRR	Material Removal Rate
PECF	Pulsed Electrochemical Finishing
PIRa	Percentage Improvement in Arithmetical Average Roughness
PIRy	Percentage Improvement in Average Maximum Height

Chapter 1

Introduction

This chapter provides a brief overview of additive manufacturing (AM), its advantages and limitations, importance of surface finishing of addictively manufactured components and different types of surface finishing processes. It also provides details about tibial tray. This chapter concluded with the organization of the thesis.

1.1 Introduction to Additive Manufacturing

Additive Manufacturing is defined as a process of joining materials to make objects from the data of 3D computer aided design (CAD) model, usually layer upon layer, as opposed to subtractive manufacturing processes". AM process is also referred to as 3D printing, freeform manufacturing, additive fabrication, or toolless manufacturing process. A CAD model is created using design software and exported to stereolithography (STL) file format that is read by the AM equipment.

AM processes can produce customized components of different metallic materials such as stainless steels, titanium alloys, nickel-based superalloys, aluminum alloys. This is applicable in aviation, aerospace, and biomedical industries.(Pant et al., 2021) Even though technological advancements have produced additive manufacturing (AM) components with fundamental mechanical and structural properties that are nearly identical to those of manufacture by conventional processes, there is still a significant barrier to the process expansion because of the parts produced by AM having higher surface roughness. As a result of the surface flaws, it deteriorates the functional characteristics of components, becoming more susceptible to corrosion and fatigue failure, which are incompatible with the applications for which it is intended. Deploying AM in industry requires the use of finishing processes to enhance surface integrity. It is a substantial cost item and an essential link in the value chain.

1.1.1 Advantages of Additive Manufacturing

The advantages of the AM processes are as follows:

- **Design Flexibility**: The complex geometries and designs can easily be manufactured by AM, which are difficult to manufacture using conventional processes.
- **Reduced Material Waste**: Additive manufacturing produces components layer by layer while only utilizing the minimal quantity of material, minimizing waste as shown in Figure 1.1 (a) and (b).
- **Environment benefits:** AM offers many positive environmental benefits in comparison to traditional manufacturing such as waste reduction and energy savings. The AM processes, compared to traditional manufacturing, are more efficient and significantly reduce the

environmental impact of waste products. They offer greater material efficiency because they only use what is needed to create a product.

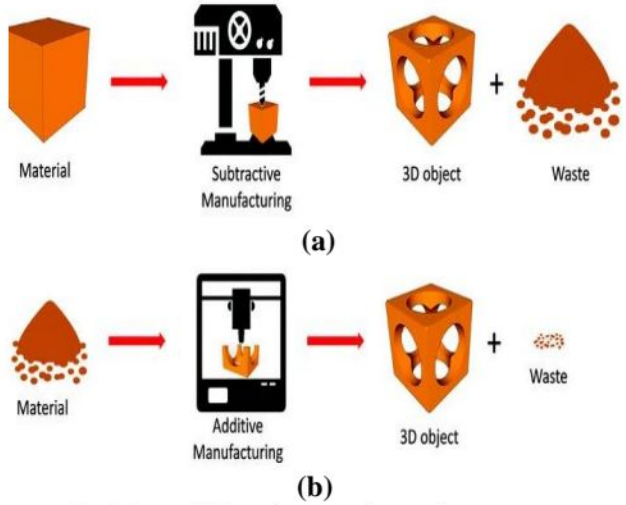

Fig 2.1: Material waste in (a) traditional manufacturing processes and (b) additive manufacturing process.

1.1.2 Limitations of Additive Manufacturing

Following are the limitations of the AM processes:

- **Material limitation:** due to layer adhesion, melting and thermal properties of some materials such as composites become difficult to employ in additive manufacturing.
- **Lower Production rate**: When it comes to mass production, additive manufacturing is typically slower than traditional manufacturing processes, due to its layer-by-layer deposition of material.
- **Poor manufacturing accuracy:** The layered manufacturing strategy of AM processes ignores the edge shape in a single layer in the spatial direction to fit the real surface curvature. The layered structure on the surface is not ignorable.
- **Post-processing requirements:** Generally, AM processes are not net-shape manufacturing processes but only a core step of the process. The AM manufactured component requires further processing to be a functional product.

1.1.3 Applications of Additive Manufacturing

- **Medical Implants**: In Orthopedic, dental, and cranial implants. These implants can be fabricated to precisely match the anatomy of each patient.
- **Aerospace Components**: Aerospace companies may use additive manufacturing to make components lighter, which boosts performance and improves fuel economy.
- **Automotive Parts**: Prototypes and finished parts may all be produced using additive manufacturing in the automobile industry, resulting in faster development times and lower expenses.

- **Food and Industry**: The food sector may employ additive manufacturing to produce customized food items, and elaborate food decorations offering consumers aesthetically pleasing experiences.
- **Architecture and Construction**: The prototypes and components of buildings may all be created using additive manufacturing. It enables more design flexibility and sustainability by producing specialized building parts.

1.2 Types of AM Process

Figure 1.2 describes different types of process involved in additive manufacturing where our focus is on selective laser melting (SLM).

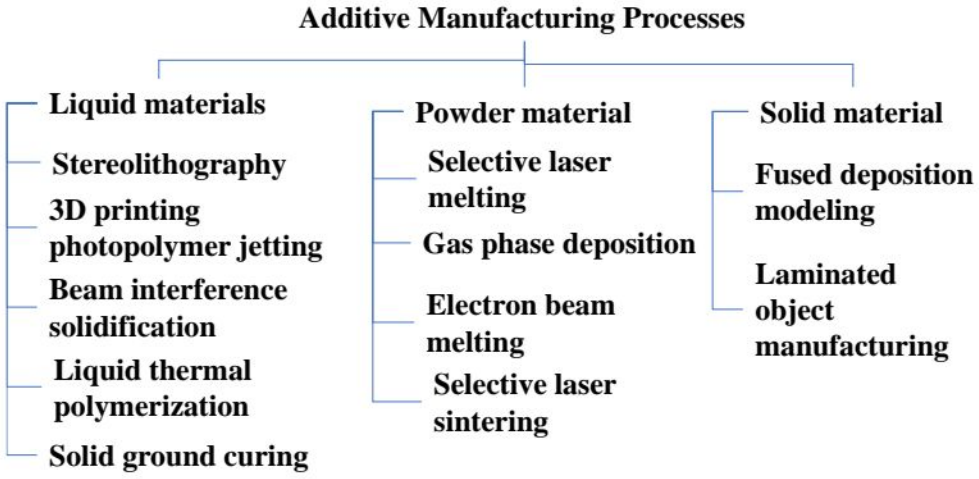

Fig. 1.2: Different types of AM processes

1.2.1 Selective Laser Melting

Figure 1.3 depicts the schematic of SLM process. A powerful laser is used in the selective laser melting (SLM) to fuse and melt powdered materials together layer by layer to produce three-dimensional objects. When employed exclusively with metal particles, SLM is sometimes referred to as direct metal laser melting (DMLM) or laser powder bed fusion (LPBF). In the SLM, a build platform is covered by thin layer of evenly distributed metallic material in powder form. The powdered particles are then selectively scanned with a powerful laser and melted in accordance with CAD (computer-aided design) model. An additional layer of powdered material is applied after the swiftly solidifying molten material to create a solid layer. Until the entire product is constructed, this process is repeated layer by layer, with each layer fusing to the one before it to produce a completely dense and solid 3D shape.

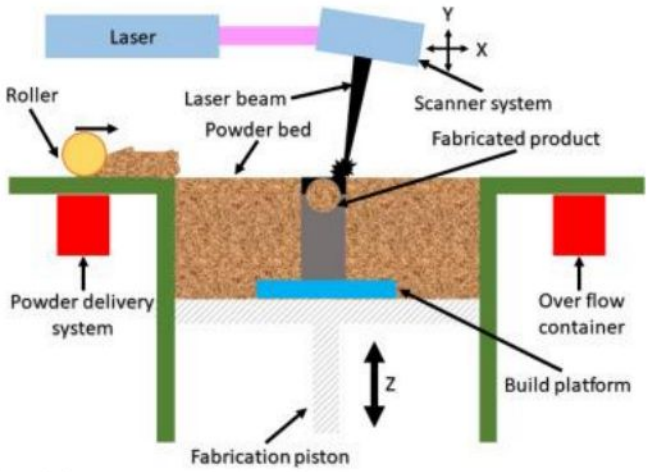

Fig. 1.3: Schematic for selective laser melting process.

1.3 Importance of Surface Finish of Components

In a variety of sectors and uses, the component surface finish is crucial. These are some of the main justifications of the importance of surface finish.

- **Functionality**: A component's performance and usability can be significantly impacted by its surface quality. For instance, precise surface finishes are required for parts in the automotive and aerospace sectors to ensure maximum performance and durability.
- **Cleanliness and hygiene**: The finished components are significant such as in the manufacture of pharmaceuticals, food processing machinery, and medical devices. Smooth and finished surfaces are simpler to clean and sterilize and can stop the buildup of pollutants or germs assuring regulatory standards.
- **Aesthetics**: Consumer items where aesthetics is important, such consumer electronics, automobile interiors, and household appliances, frequently include surface finish as a key component. A better surface finish may improve a product's look and perceived value, which can play a significant role in consumer choice.

1.4 Introduction to Tibial Tray

In knee replacement surgery, the tibial tray is a tool utilized. It is a component of the implant system that fixes the tibial plateau, the top of the tibia (the shin bone), where it connects to the femur (thigh bone) for forming the knee joint. The tibial tray works as a medium where tibial inserts, a cushion-like piece of metal or plastic, articulates with the femoral component to allow for fluid motion of the knee joint. To suit diverse surgical procedures and patient anatomy, tibial trays are often composed of metal or high-density polyethylene (HDPE). Based on the type of knee replacement, they are often press-fit or fastened to the tibia using bone cement. The tibial is inserted in the region that has been prepared during knee replacement surgery after the damaged bone and cartilage of the tibial plateau have been removed. (Peto et al., 2019)The femoral component is then linked to the femur, and the tibial insert is then joined to the tibial tray, creating a new joint surface that enables patients with knee joint arthritis or other disorders that call for knee replacement surgery to function better and experience less discomfort.

1.5 Process Used in Manufacturing Tibial Tray

- **Design**: A tibial component is designed by computer-aided design software before being manufactured. The design contains requirements like size, form, and material choice. Fig. 1.4 depicts its picture.
- **Material selection**: Components for tibial composed of biocompatible polymers or metals like titanium or cobalt-chromium alloys.
- **Raw material preparation**: Once a material being chosen, it is procured in raw form and put through preparation procedures like casting, forging, cutting to give it the shape.
- **Machining**: To eliminate extra material and produce the final shape of the produced material is next processed using computer numerical control with maintained high accuracy.
- **Surface treatment**: Processes like grinding, polishing, or coating the tibial component's surface can be used to increase its wear resistance and decrease friction to improve performance.
- **Quality control**: Procedures used in the production process to guarantee that the component complies with the requirement which involves checking the component's size, material composition, and performance traits.
- **Packaging and sterilization**: Then after passing quality control, it is stored in a sterile container to keep it intact until it is needed in surgery. To ensure it is free of hazardous germs.
- **Distribution**: After sterilization, the tibial component is supplied to medical institutions and hospitals where it is stored until it is required for a knee replacement procedure.

Fig. 1.4: Photograph of Knee implant and its components.

1.6 Types of Surface Finishing Process for Amed Components

There are different types of surface finishing process of which few of them are described as follows:

1.6.1 Pulsed Electrochemical Finishing (PECF)

Electrochemical finishing (ECF) reduces the surface roughness by removing more material from surface peaks of anodic workpiece by controlled electrolytic dissolution governed by Faraday's laws

of electrolysis. It is also known as electrochemical polishing, anodic polishing, or electrolytic polishing. The diagram in Fig. 1.5 shows its process.

Reasons to select PECF: It is a non-contact finishing process which gives stress free surface and good surface finish and allows finishing of fragile and delicate parts.

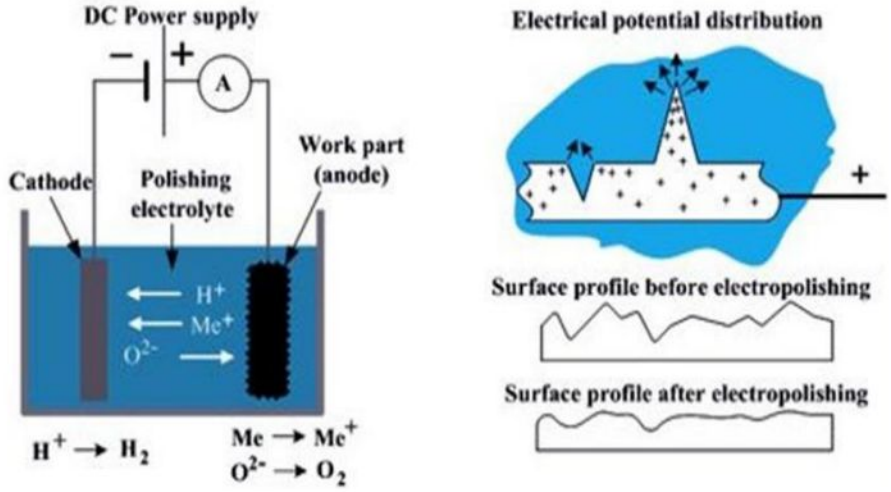

Fig. 1.5: Schematic of PECF process.

Process Principle of PECF for Surface Finishing

The actual working principle of PECF process is explained by **Ma et al. (2010)** where a typical PECF setup includes immersing the workpiece in electrolytic solution and positioning a tool or electrode near the workpiece surface. (Bryant, 2019) An electrochemical reaction occurs when an electric potential is introduced between the workpiece and the electrode, resulting in the material dissolution from the workpiece surface. However, with PECF, the current is administered in a pulsing way, with regulated on/off cycles, resulting in a pulsating material removal action. This pulsing motion aids in managing the pace of material removal, and the electrolyte flow may be adjusted to flush away dissolved material and avoid re-deposition, resulting in enhanced surface quality.

1.6.2 Magnetic Abrasive Finishing (MAF)

Magnetic abrasive finishing, also known as magnetic abrasive deburring (MAD) or magnetic abrasive finishing (MAF) is a surface finishing method that employs a combination of magnetic fields and abrasive particles to remove material from a workpiece and achieve desired surface quality. The diagram in Fig. 1.6 shows its process.

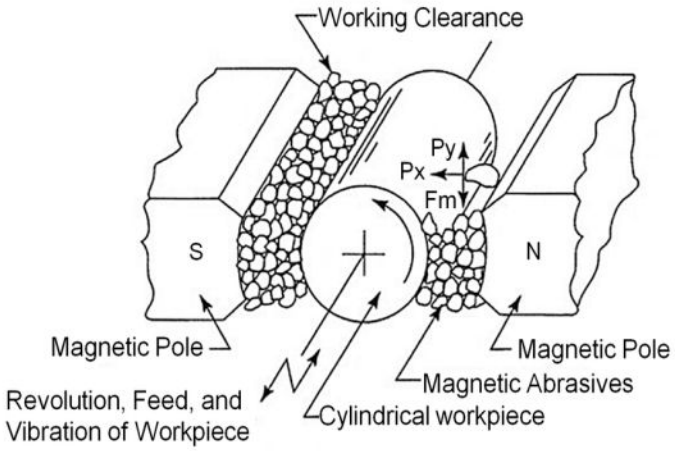

Fig. 1.6: Image showing magnetic abrasive finishing.

1.6.3 Hydrodynamic Cavitation Finishing (HDCF)

Hydrodynamic cavitation finishing, also known as acoustic cavitation or ultrasonic cavitation is a specialized surface finishing method that uses the cavitation phenomena to improve the surface qualities of materials. The diagram in Fig. 1.7 shows its process.

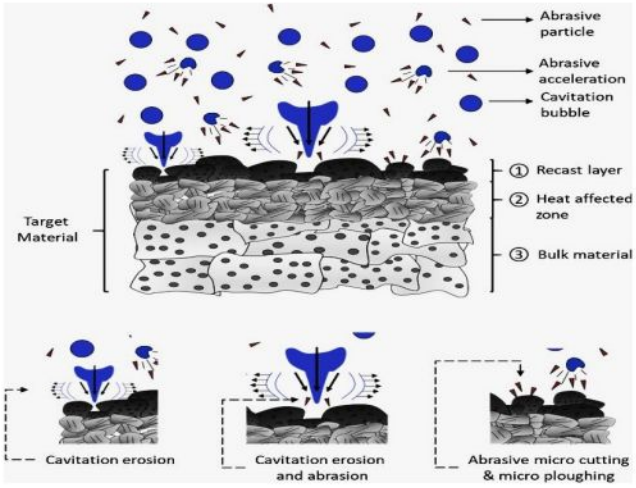

Fig. 1.7: Image showing hydrodynamic cavitation finishing.

1.6.4 Centrifugal Tumble Finishing (TF)

Centrifugal tumble finishing is a mechanical surface finishing method that includes inserting components or media into a spinning container, typically a vibratory bowl or barrel, with abrasive media, water, or cleaning solutions. The container is then placed in motion, forcing the components and media to tumble, crash, and rub against one another to provide the required surface finish. . It involves several stages like roughening, smoothening, and polishing. The diagram is shown in Fig. 1.8.

Fig. 1.8: Image showing centrifugal tumble finishing.

1.6.5 Wire electrical discharge finishing (WEDF)

WEDF is a specialized Finishing method that uses the principles of electrical discharge machining (EDM) to produce high-precision polishing of hard and brittle materials such as metals, ceramics, and composites. WEDF is frequently used in sectors requiring tight tolerances and excellent surface finishes. (Ogawa et al., 2020)Figure 1.9 shows its process diagram.

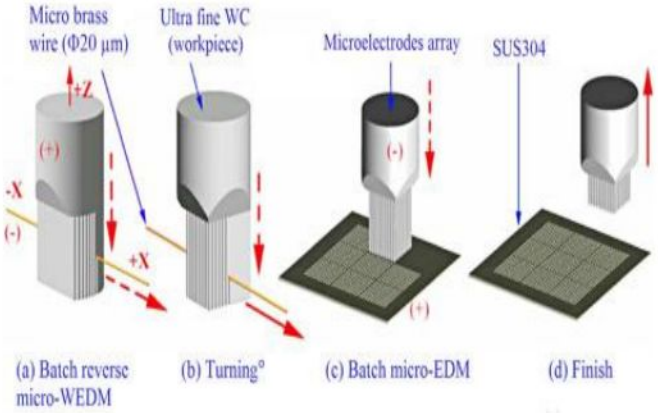

Fig. 1.9: Image showing WEDF process.

1.7 Organizations of the Thesis

This thesis is organized into five chapters with following contents:

Chapter 2 presents a review of past work on PECF of SS316 L alloy, research gaps identified based on this review and the research objectives defined based on the identified research gaps.

Chapter 3 presents fabrication of finishing chamber and subsystems of the experimental setup and planning and details of experiments carried out for the present work. It also presents the experimental procedure.

Chapter 4 presents experimental results and their analysis focusing on the effects of variable input parameters of PECF process on workpiece along with identification of optimum level of the process parameters.

Chapter 5 highlights the conclusions derived from the present work and scope for future work based on the limitations of the present work.

Chapter 2

Review of Past Work

This chapter discusses prior research on the use of various metallic materials for knee implant applications, the creation of high entropy alloys for use in knee implants, the manufacture of knee implants using additive manufacturing (AM) processes, a summary of pertinent prior research, gaps and research objectives that were identified, and the methodology applied to achieve those objectives.2.1 Past work on finishing of workpiece by PECF

2.1 Past Work on Finishing of Workpiece by PECF

ECF has reported limited work on finishing gears, while PECF has reported even less work on finishing gears. **Wang et *al.* (2016)** have presented review on its efforts on finishing of SS316L. The following paragraphs summaries previous work done using ECH and PECH for gear finishing. **Ma and Tao (2010)** explore the application of (ECF) and (ECM) to improve workpiece surface quality. The research proposes an idealized statistical model for determining finishing process results and compares them to experimental findings acquired using a Tal surf profilometer. As per the findings, PECF is an efficient approach for minimizing surface roughness and enhancing surface quality. The model can understand the anodic smoothing and accurately forecast the results. PECF is an effective strategy for increasing workpiece surface quality. The model in the study may be employed for regulated PECF operation and reasonably accurate prediction of results. **Taylor and Inman (2014)** highlight an innovative technique to ECF that use pulse and pulse reverse electric fields to obtain the surface finish while using ecologically friendly chemicals. This reduces production costs while increasing process resilience. The mechanistic aspects of pulse/pulse reverse surface finishing processes lack fundamental understanding. The publication includes case studies on deburring automobile gears as well as electropolishing semiconductor valves and superconducting radio frequency cavities. **Mohammad and Wang (2016)** used ECF to improve surface quality and mechanical qualities. The essential factors influencing ECM polishing process, such as applied voltage, electrolyte concentration, rotating speed, and polishing pressure examined. Several modifications to the traditional ECF process are proposed including electrochemical mechanical polishing robotic systems, robotic electrochemical grinding systems, robotic electrochemical with burnishing force systems, and robotic electrochemical polishing systems with assistive magnetic fields. The benefits of each suggested design are examined, as are future research and industry demands. **Gallegos et *al.* (2017)** presents the experimental investigation of the

parameters impacting the surface finish of ECM machined SS316 samples. Parameters such as electrolyte flow rate, voltage gap and electrolyte temperature were all adjusted. The findings revealed a substantial link between overpotential and surface finishing. The overpotential is affected by the current density electrolyte properties and current density. (Wu et al., 2001)As a result, conductivity, electrolyte flow rate and intake temperature have a direct impact on surface finish. To achieve the desired reflective and brilliant surface quality, between 9 and 15 V potential is required. **Ogawa et *al.* (2020)** describes how workpiece thickness affects characteristics of machining by WECM finishing. Also, the impacts on surface roughness Ra, machining depth, and completed surface straightness. The study investigates the machining properties under various electrolyte concentrations and softening of wire via Joule heat production. The researchers discovered that decreasing the electrolyte content resulted in minimum surface roughness at the same machining depth. It states that by modifying the outlet form of the slit nozzle, the current-feeding part can be reduced, and the electrolyte-jetted section may be increased that does not soften or break the wire even at high currents. **Douche et *al.* (2022)** presents results relating to the electropolishing of high roughness 316 L SLM components. The polarization curves produced on inclined and horizontal raw SLM samples show normal electropolishing behavior. The roughness development versus treatment potential plot demonstrates a building direction dependency, with inclined surfaces reacting better to the levelling phenomena. In comparison to the initial roughness, the final roughness after 20 minutes of electropolishing was found to give better results. As the potential increases on the polishing plateau, the dissolution rate measured experimentally ranges between 3.5 and 5 m/min. **Kumar and Dixit (2023)** examine electrochemical jet machining (ECJM) use as a surface finishing procedure for additively produced (AM) parts after processing. The study studies the phase analysis, surface morphology, elemental composition, and surface roughness before and after the finishing operation and focuses on the influence of process parameters on the surface roughness. The study shows that the ECJM method successfully eliminates surface imperfections and flaws, resulting in smooth post-finished samples with uneven humps and few stray corrosions left previously by big molten pool overflows. The optimized ECJM process settings lower the average surface roughness and peak-to-valley roughness by 72% and 61%, respectively.

2.2 Summary of the Past Work

Following conclusions can be drawn from the review of the relevant past work described in the previous sections:

- Although AM processes like SLM have demonstrated tremendous potential to produce high-quality knee implants, they are also constrained by some intrinsic issues such as thermal distortion heat-affected zone, energy consumption, thermal distortion and higher production and maintenance costs.
- The μ-PAAM process appears to have significant potential for environmentally and economically manufacturing knee implants, is energy-efficient, economical, and environmentally benign.
- A low-carbon version of stainless steel 316, noted for its high temperature strength and superior corrosion resistance is known as SS316L. It has molybdenum, which increases its ability to withstand corrosion caused by numerous substances, particularly chlorides.(Rotty et al., 2019)
- Compared to other popular electrolytes, sodium nitrate ($NaNO_3$) has a low electrical conductivity. Large concentration of sodium nitrate ($NaNO_3$) showed lower rates of material and lower electrolytic reactions removal during the finishing process whereas this does not happen in case of sodium chloride (NaCl) as it showed better material removing properties.

2.3 Identified Research Gaps

Based on a study of previous work on the surface finishing by PECF method, the following research needs were identified:

- Limited studies with different tools and electrolytes for effective surface finish of additive manufactured parts by PECF process.
- No detailed study on parameters like:
- Effects of different pulse duration (T_{on} and T_{off}) on the workpiece.
- Different electrolytes affect during operation on the workpiece.

2.4 Research Objectives

Following are the research objectives from the present work:

- To improve surface finish of μ-plasma arc additively manufactured Tibial Tray (of knee implant) by PECF process.
- To identify Optimum Parameters of PECF Process through proper planning and design of experiments

2.5 Research Methodology

Figure 2.1 depicts the research approach employed to achieve the defined research objectives.

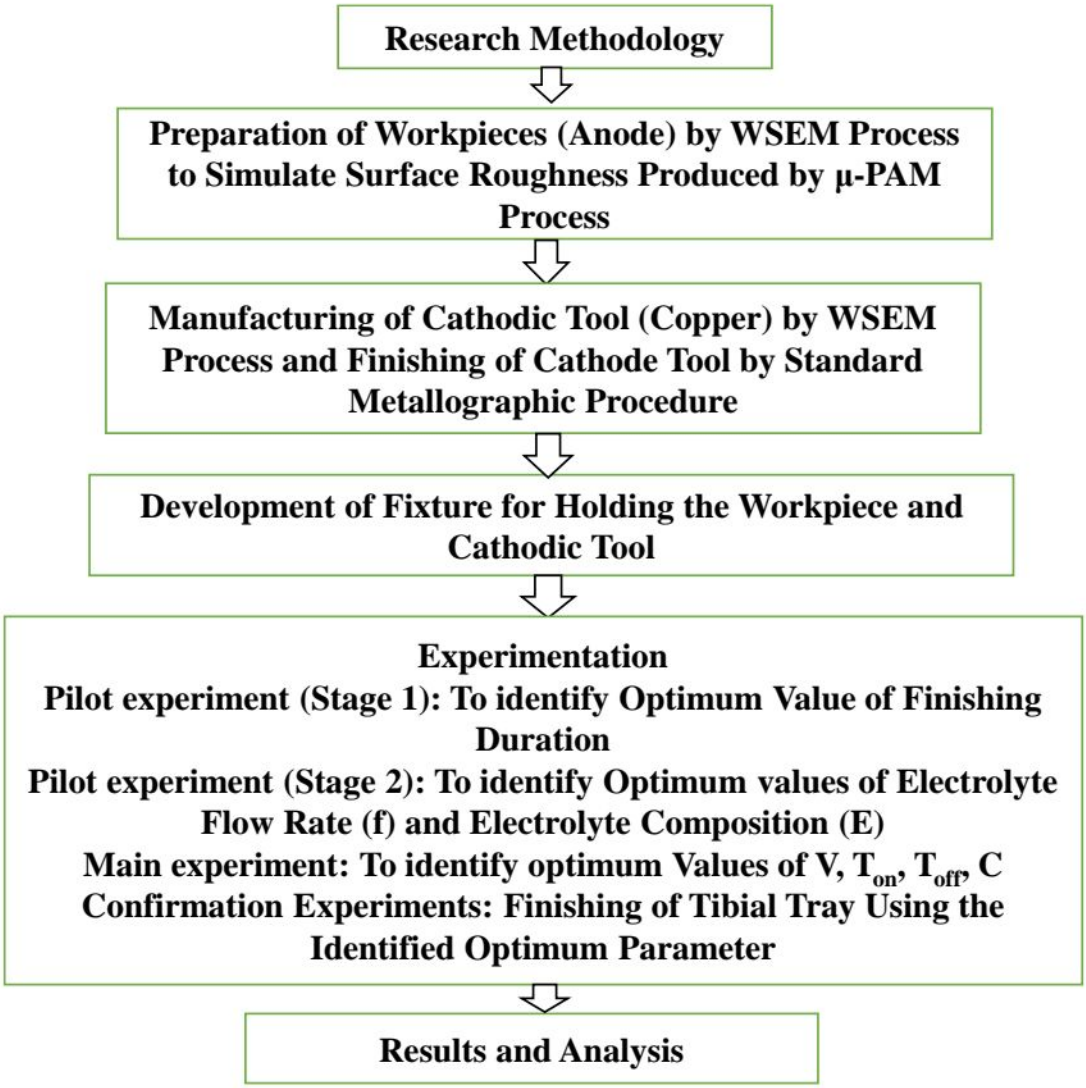

Fig. 2.1: The current work's research methodology.

The ***next chapter*** describes in detail the experimental equipment created for fine finishing the AM component using the PECF technique.

Chapter 3

Experimentation and Design of Experiments

This chapter discusses the approach to various experimental procedures, apparatus, materials involved in the experimentation and the design of the experiments to make those experiments compatible with the different parameters.

3.1 Development and Details of the Experimental Apparatus

An experimental apparatus for simultaneous advancement in surface finish and finishing productivity of the tibial component was established for running PECF operations. The following enhancements can be made to increase the performance of electrochemical finishing apparatus:

- High-precision control system
- Improved electrode design
- Real-time monitoring and feedback
- Environmentally friendly electrolyte solutions
- Higher efficiency power supplies
- Improved safety features

Tooling system includes Power supply system, electrolyte supply and cleaning system, cathodic tool system, finishing chamber

3.1.1 Power supply system

A low DC voltage in the range of 4-30 volts with current adjustable up to 50A is supplied over the inter electrode gap (IEG) between the cathodic tool and anodic workpiece. This gap is flooded with a suitable electrolyte. To supply the current in the IEG, a computer-controlled DC power supply unit (model 3300 W DC power supply) with the producing an output voltage in the range of 0-100 V for low voltage units and high voltage 0-660 V for high voltage applications, a current in the range of 10-110 A, and computer controlled programmable options for setting pulse-on time and pulse-off time was used. It contains a programmable sequencer that may be used as a random waveform generator and to construct loops and ramps, and it is controlled via Ethernet programming. This enables it to provide continuous and DC power supply with pulses for the electrolytic dissolving process, as well as flexibility in picking the most suited settings based on the process's requirements (Ishimoto et al., 2021). It displays the rise and fall time figures, which reflect the process takes place in real time. Figure 3.1 represents the schematic diagram of the experimentation procedure

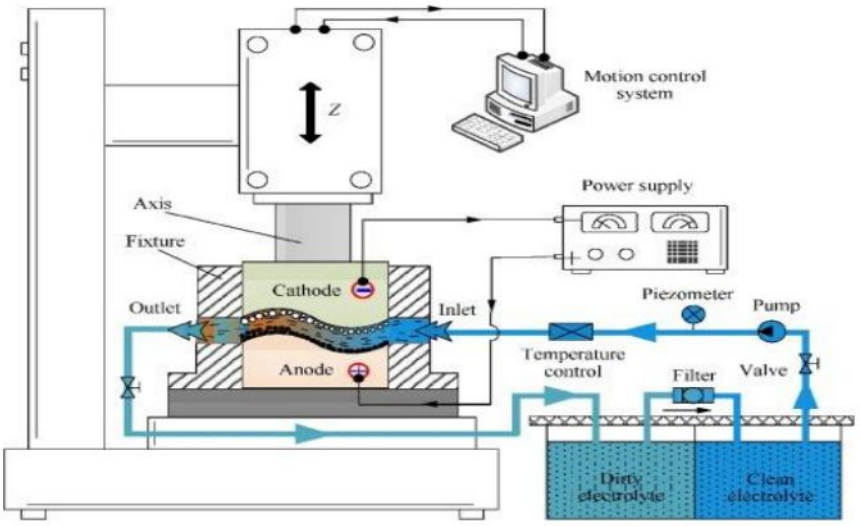

Fig. 3.1: Schematic for Electrochemical Finishing Process.

3.1.2 Electrolyte Supply and Cleaning System

The supply of electrolytes and recirculating system comprises of an electrolyte storage tank, a settling tank, a stainless-steel pump (Fig. 3.4a), electrolyte carrying tubes, a flowmeter, flow control valves, and devices to maintain constant temperature. It was intended to recycle the electrolyte to the finishing chamber at the proper flow rate and temperature. Given the materials of the workpiece, and cathode tool, an aqueous combination of sodium chloride (NaCl) and sodium nitrate (NaNO3) was chosen as the electrolyte considering the materials of workpiece and cathodic tool. To store and deliver the electrolyte, a 300-liter PVC storage tank was employed. The storage tank's elevation was kept high enough to enable a steady supply of electrolyte for the pump to start and a natural head for free return of the electrolyte from the chamber. The electrolyte supply system includes two double stage stainless steel filters and magnetic filters installed in the electrolyte flow channel to clean the electrolyte and assure its purity. the flow of electrolyte is measured using a rotameter.

Selection of the Electrolyte: NaCl and $NaNO_3$

Reasons for selecting NaCl and $NaNO_3$ as an electrolyte:

- **NaCl:** As this electrolyte is abundantly and easily available at a low cost which gives a high material removal rate (MRR). It has high solubility, compatibility, stability with low toxicity, and predictable behavior. Most importantly, it is eco-friendly.
- **$NaNO_3$:** This electrolyte is reliable and versatile and has good conductivity, stability, solubility and is non-toxic.

3.1.3 Manufacturing of Cathode Tool

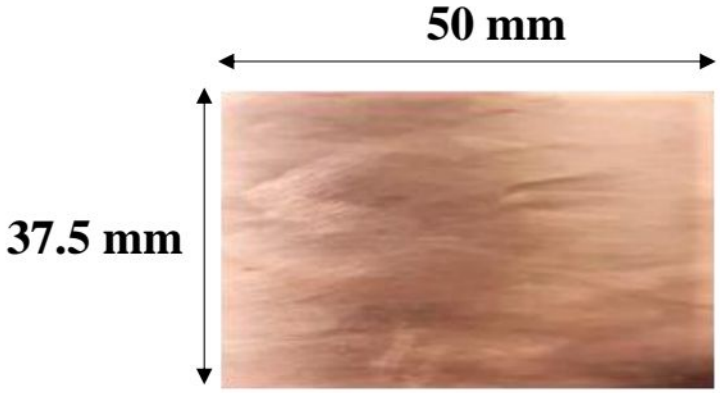

Fig. 3.2: Cathode tool and its dimensions.

.

Manufacturing of Cathodic Tool (Copper) shown in figure 3.2 was done by WSEM Process. Finishing of Cathode Tool was done by Standard Metallographic Procedure. Polishing of copper tool with polishing machine, emery paper of different grit sizes of 200, 500 and 1000 along with hifin diamond fluid spray for reflection of better polishing effect. The Identified arithmetical average roughness before polishing 'Ra' 9.112 µm and average maximum height 'Ry'36.24 µm and the identified arithmetical average maximum height after polishing 'Ra' 3.12 µm and average maximum height 'Ry'8.74 µm. It has the thickness of 5.7 mm. Copper was selected Due to its high conductivity, high electrochemical stability, easily available and good mechanical properties.

3.1.3.1 Manufacturing of Anodic Workpiece

The different composition of the workpiece that is SS316L is shown in the Table 3.1

Table 3.1: Chemical Composition of SS316L Alloy (Wt. %)

Constituents	C	Mn	P	S	Si	Cr	Ni	Mo	N	Fe
Weight %	0.03	2.0	0.045	0.03	0.75	16.0	10.0	2.0	0.10	Bal.

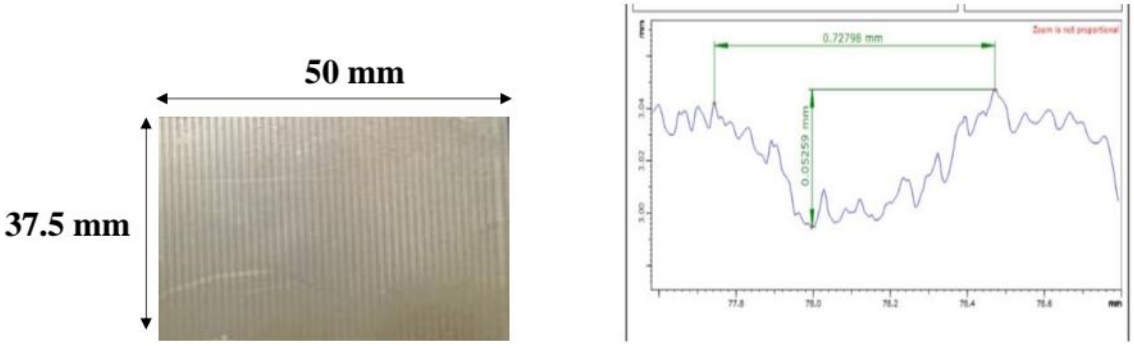

(a) **(b)**

Fig. 3.3: (a) Anode workpiece and its dimensions (b) grooves showing its width and depth.

Preparation of Workpieces (Anode) was done by WSEM Process to Simulate Surface Roughness Produced by μ-PAM Process. Created grooves were created with having the width 0.052 mm and depth 0.0727 mm shown in figure 3.3 (a) and (b). Total samples of workpiece prepared was fifty on having thickness of 3mm. This material has been selected as it is excellent corrosion resistance, high strength, and durability, easy to fabricate, hygienic and safe and aesthetic appealing.

3.1.3.2 Development of Fixture

Fig. 3.4: Design of the fixture

Acrylic Perspex sheet shown in figure 3.4 is used in developing the fixture material. Fixture manufactured by the horizontal milling machine with hole diameter 4.5mm. Total length 60 mm and width 40.5 mm. This material is chosen as it is transparent that one can see the experiment happening and it is strong.

3.1.4 Finishing Chamber

The main goal of the experimental apparatus was to design and build the appropriate tooling setup i.e., finishing chamber and cathodic tool. It consists of (i) a specifically cathodic tool (made of copper) sandwiched in the fixture for electrolyte dissolving while maintaining the appropriate IEG. (ii) the workpiece (made of stainless steel) that will be completed using the PECF process (iii) support and mounting arrangements for the workpiece and cathode (iv) provision for providing DC pulse power between the workpiece and the cathodic tool (v) a fixture (made of Perspex sheet) is mounted on a wooden block under which the anodic workpiece and cathodic tool was inserted.

Because PECF is a combination of electrochemistry and ECM and involves electrolyte, electrical equipment, and mechanical scrubbing, the design and material selection for various elements of the apparatus's elements which are based on various key aspects such as electrical conductivity, anti-corrosiveness, manufacturability, economics, and so on.

Experimental Apparatus The different experimental apparatus used in the setup for the conduction of PECF experimentation is shown in Fig. 3.5 (a), Fig. 3.5 (b), Fig. 3.5 (c), Fig. 3.5, (d) and Fig. 3.5 (e).

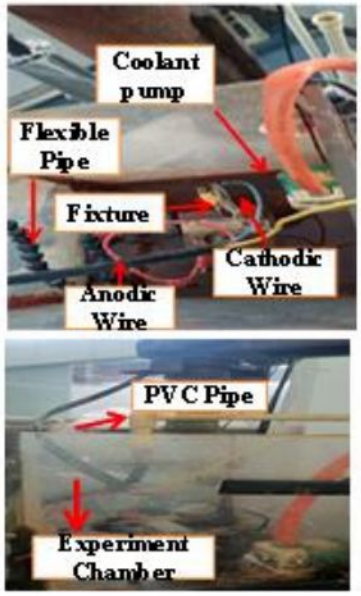

(a)

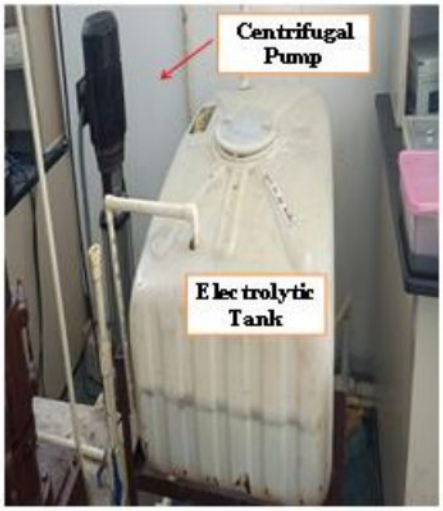

(b)

(c)

(d)

(e)

Fig 3.5: Experimental apparatus developed for finishing of workpiece by PECF (a) Finishing chamber, (b) Electrolytic tank, (c) Photograph of the oscilloscope, (d) Rotameter to measure flow rate, and (e) stainless-steel centrifugal pump.

3.2 Design and Planning of Experiments

Experiments were developed in accordance with the study purpose utilizing a statistical method to design experiments. A full-factorial method was used to design the experiments at 1st stage of pilot experiment by varying the parameters: applied voltage, concentration, IEG, electrolyte flow rate, pulse on time, pulse off time and constant parameter was finishing duration. Similarly, in the 2nd stage of pilot experiment, the varying parameters were composition and flow rate of electrolyte and constant parameters were voltage, pulse on time, pulse off time and concentration. Then, in the main experiment, Box-Behnken design method was implemented by varying the parameters voltage, pulse on time, pulse of time and concentration of the electrolyte to determine all the optimum values from all the stages of experiment for performing the final confirmation experiment by PECF method. To establish cause-and-effect correlations, the design of experiments is a systematic way to ascertain the relationship between elements influencing a procedure as well as its results. To manage the inputs to the process and maximize the output, this information is required. The following are the main DOE strategies.

Full Factorial Design: An experiment with a full factorial design is one whose experimental units include every possible combination of all potential across all such levels factors, each of which has a discrete possible level. With the use of such an experiment, it is possible to examine how each element affects the response variable as well as how different factors interact with one another. The experimental setup where each input factor has two levels is a popular one.

3.2.1 Box-Behnken Design Method

In engineering and statistics, the Box-Behnken Design kind of experimental design is frequently employed. It uses a statistical method called a response surface method to optimize a system's output based on its input variables. Each factor is adjusted at three separate levels in the three-level, three-factor Box-Behnken Design. The levels are selected in a manner that prevents the design points from being on the margins of the design environment, which can interfere with extrapolation. The design is made up of several points that are selected in a way that allows it to be rotated, making it possible to estimate the curvature of the response surface and fit a second-order polynomial to the data. The following are some benefits of using this BBD approach: a) Reduced number of experiments b) good coverage of experimental space 3) Robustness to model assumptions d) Easy to execute e) Efficient optimization. Thus, The Box-Behnken Design is overall an effective method for experimental design and optimization that enables researchers to quickly explore the design space and get the best outcomes.

3.2.2 Details of Experiments

Fifteen experiments were planned and performed using full factorial approach for design of experiments in pilot stage 1 where five experiments are conducted on four samples i.e., total twenty experiments to determine the finishing duration at different time intervals as 5, 10, 15, 20, 25, 30 minutes as a part of time dependent study in PECF with varying parameters including applied voltage, concentration, IEG, electrolyte flow rate, pulse on time, pulse off time and constant parameter was finishing duration.

3.2.3 Design of Pilot Experiment Stage-1

Fifteen experiments were planned and performed using full factorial approach for design of experiments in pilot stage 1 where five experiments are conducted on four samples i.e., total twenty experiments to determine the finishing duration at different time intervals as 5, 10, 15, 20, 25, 30 minutes as a part of time dependent study in PECF with varying parameters including applied voltage, concentration, IEG, electrolyte flow rate, pulse on time, pulse off time and constant parameter was finishing duration. The measured responses were arithmetical average roughness *'Ra'* (µm), average maximum height *'Ry'* (µm), Material removal rate, volumetric MRR' (mm^3/s). The parameters used is shown in Table 3.2.

Table 3.2: Parameters used to identify the finishing duration through time dependent study.

Constant Parameters	**Used Values**
Electrolyte	Aqueous solution of NaCl
Applied Voltage, '*V*' (volts)	15
Concentration, '*C*' (%)	5
Interelectrode gap, 'IEG' (mm)	1
Electrolyte flow rate, '*F*' (l/min)	10
Pulse-on time, 'T_{on}' (ms)	3
Pulse-off time, *'T_{off}'* (ms)	4
Variable Parameter-	
Finishing Time '*t'* (Minutes)	5, 10, 15, 20, 25

3.2.4 Design of pilot experiment Stage-2

Similarly, in the 2nd stage of pilot experiment also full-factorial approach was implemented for three flow rates and five composition ranges of electrolyte hence, fifteen experiments are performed here. The varying parameters were composition and flow rate of electrolyte and constant parameters were voltage, pulse on time, pulse off time and concentration. Here, the composition and flow rate of electrolyte values were to be optimized. This is a full factorial design with a total of fifteen experiments. The parameters used in this stage are shown in Table 3.3.

Table 3.3: Parameters used to deduce values of flow rate and composition of the electrolyte

Variable Parameters	Values	Constant Parameters	Values
Composition ($NaCl + NaNO_3$)	100% NaCl	Voltage (volts)	20
	75% NaCl + 25% $NaNO_3$	Pulse on time, 'T_{on}' (ms)	3
	50% NaCl + 50% $NaNO_3$	Pulse off time, Toff (ms)	4
	25% NaCl + 75% $NaNO_3$	Concentration, C (%)	5
	100% $NaNO_3$		
Electrolyte flow rate (l/min)	10,15,20		

3.2.5 Design of Main Experiment

Then, in the main experiment, Box-Behnken design method was implemented. Total twenty-seven experiments are conducted by varying the parameters voltage, pulse on time, pulse of time and concentration of the electrolyte at different levels to determine all the optimum values from the varying parameters to use it in the final confirmation experiment by PECF method.

To identify optimum values of applied voltage, Pulse on time, Pulse off time, Concentration of electrolyte which is varying parameters as shown in Table 3.4 and constant parameters used were finishing duration, flow rate and composition of the electrolyte.

Table 3.4: Box-Behnken design of experiments with four parameters Conc, V, T_{on} and T_{off}

Exp. no.	Concentration of the electrolyte (C)		Applied Voltage (V)		Pulse on time 'T_{on}' (ms)		Pulse off time, 'T_{off}' (ms)	
	Coded	*Actual*	*Coded*	*Actual*	*Coded*	*Actual*	*Coded*	*Actual*
1	0	5	0	25	1	3	-1	6
2	1	10	1	30	0	2	0	2
3	0	5	1	30	0	2	1	4
4	0	5	0	25	1	3	1	4
5	-1	15	0	25	0	2	-1	6
6	-1	15	-1	20	0	2	0	2
7	1	10	-1	20	0	2	0	2
8	0	5	0	25	0	2	0	2
9	0	5	-1	20	0	2	-1	6
10	0	5	0	25	0	2	0	2
11	0	5	1	30	0	2	-1	6
12	-1	15	0	25	0	2	1	4
13	0	5	-1	20	1	3	0	2
14	0	5	1	30	1	3	0	2
15	0	5	0	25	-1	4	1	4
16	0	5	1	30	-1	4	0	2
17	0	5	-1	20	0	2	1	4
18	1	10	0	25	-1	4	0	2
19	1	10	0	25	1	4	0	2
20	0	5	-1	20	-1	4	0	2
21	1	10	0	25	0	2	1	4
22	-1	15	1	30	0	2	0	2
23	-1	15	0	25	-1	4	0	2

24	1	10	0	25	0	2	-1	6
25	0	5	0	25	-1	4	-1	6
26	-1	15	0	25	1	3	0	2
27	0	5	0	25	0	2	0	2

After deriving the optimized values from the main experiment, it was further used in the confirmation experiment to perform PECF on the tibial part and three other samples on the four varying parameters which are shown below in the table.

3.2.5.1 Confirmation Experiments

To identify Surface finish of μ-PAM Manufactured Tibial Tray using identified optimum values of *'T_f', 'F', 'C', 'V', 'T_{on}', 'T_{off}'* as shown in Table 3.5 and constant parameters be finishing duration, flow rate and composition of the electrolyte.

Table 3.5: Different varying parameters and its optimized values

Parameters	**Optimized Values**
Applied Voltage, *'V'* (volts)	25
Pulse on time, *'T_{on}'* (ms)	4
Pulse off time, *'T_{off}'* (ms)	6
Electrolyte Concentration, *'C'* (%)	15

3.3 Measured Responses

Below are the measured responses which were determined after conducting the PECF experimentation at different parametric levels.

3.3.1 Evaluation of Surface Roughness

The surface quality is strongly impacted by surface roughness. (Mohammad and Wang, 2016)Three surface roughness metrics, including average roughness (Ra), maximum roughness (R_{max}), and depth of roughness (R_z), were measured were measured using 3D optical profiler, Hand surf and LD 130 contact and non-contact surface roughness measuring machine. Measurements were taken along the surface of the workpiece showing depth and width. Material removal rate (MRR) and maximum change in percentage reduction are also measured after the experiment is conducted. After finishing by the PECF process, a roughness parameter with a larger value of the % improvement implies a lower value for that parameter.

3.3.2 Evaluation of Finishing Productivity of PECF

Every finishing process's primary concern for commercial adoption is finishing productivity. In this study, the volumetric material removal rate (MRR), shown in equation 3.1which was calculated by dividing the loss in mass of the workpiece during the PECF process by the product of finishing time and material density, was used to measure finishing

productivity. On a precise weighing machine, the weight of the finished workpiece was measured.

$$\text{MRR} = \frac{\text{Weight of workpiece before finishing (g)} - \text{weight of workpiece after finishing (g)}}{time\ duration\ (s) \times density\ of\ workpiece\ material\ (g/mm3)} \quad (3.1)$$

According to several variables, including the process parameters, the material qualities, and the beginning surface state, the percentage change in roughness shown in equation 3.2 of a surface following electrochemical finishing can alter. Therefore, the percentage change or reduction is calculated by:

$$\%\ \text{change in surface roughness} = \frac{Final\ value - Initial\ value}{Final\ value} \text{x } 100 \quad (3.2)$$

3.4 Experimental Procedure

The following method was used in all the experiments:

- For all the unfinished workpiece that would be utilized in the trials, all considered reactions were measured.
- In the electrolyte holding tank, electrolyte was created with the requisite composition and concentration. Utilizing the flow control system and temperature control unit, the electrolyte temperature and flow rate were regulated to the necessary value.
- It was made sure that the workpiece and cathode tool were properly situated in the fixture maintaining a required minimum interelectrode gap to prevent misalignment or non-uniformity.
- Electrolyte flow rate was maintained by the regulating valve and rotameter to avoid the uncertainty of flow rate.
- The applied voltage, pulse-on duration, and pulse-off time values were established in accordance with the experimental plan's specifications.
- An experiment's finishing time was determined using a stopwatch, and once it had passed, the experiment was terminated.
- The workpiece gear was thoroughly cleaned with cotton after each experiment to prevent rusting from exposure to caustic in the finishing electrolyte chamber. The cotton was then immersed in lubricating oil.
- For every sample workpiece that PECF finished measuring, all the considered responses.

The best finished samples are described in the next chapter along with their comments.

Chapter 4

Results and Discussion

This chapter examines the experiment results, summarizes them, analyses them, and draws conclusions.

4.1 Result of First Stage of Pilot Experiment

This stage shows the results of the PECF experiment on four different samples for the determination of finishing duration at time intervals of 5,10,15,20 and 25 minutes. It is a time dependent study to optimize the optimal value of the finishing duration at different samples.

Table 4.1: Results for Sample 1 of pilot stage first experiment

Finishing duration (min)	**Arithmetical Average Roughness *'Ra'* (µm)**			**Average Maximum Height *'Ry'* (µm)**			**MRR (mm^3/s)**
	Before PECF	**After PECF**	**'%' change in 'Ra'**	**Before ECF**	**After PECF**	**'%' change In 'Ry'**	
5	5.91	5.82	1	49.17	40.75	20.6	0.395
10	5.82	4.81	2.9	40.75	28.17	30.8	0.845
15	4.81	4.16	13.5	28.17	24.01	14.7	0.404
20	4.16	2.04	50.9	24.01	23.07	3.9	0.495
25	2.04	1.34	34.3	23.07	13.15	42.9	0.662

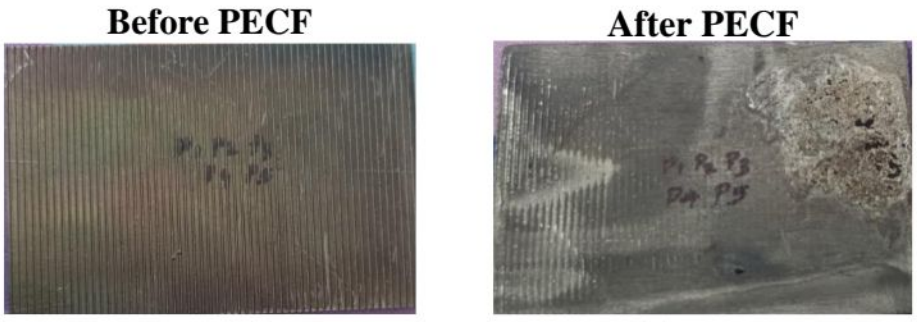

Fig. 4.1: (a) surface of sample before experiment and (b) surface of sample after experiment.

From the above Table 4.1, where the experiment has been performed on a single sample which was time dependent study starting from 5 minutes to 25 minutes. This showed that the percentage change in arithmetical average roughness *'Ra'* (µm) increased to 34.3% and percentage change in average maximum height *'Ry'* (µm) increased to 42.9%. At other finishing durations such as 5, 10, 15 and 20 minutes no such satisfactory changes were observed. The achieved minimum surface roughness of 13.15 (µm) was found at 25 minutes

finishing duration with material removal rate at 0.662 (mm^3/s). The image of the sample is shown in Fig. 4.1(a) and Fig. 4.1(b).

Table 4.2: Results for Sample 2 of pilot stage first experiment

Finishing duration (min)	**Arithmetical Average Roughness *'Ra'* (µm)**			**Average Maximum Height *'Ry'* (µm)**			**MRR (mm^3/s)**
	Before PECF	**After PECF**	**'%' change**	**Before PECF**	**After PECF**	**'%' change**	
5	6.11	5.76	5.7	53.45	40.0	25.1	0.491
10	5.76	5.43	5.7	40.00	35.29	11.7	0.650
15	5.43	4.48	17.4	35.29	28.70	18.6	0.404
20	4.48	1.59	64.5	28.70	14.29	50.2	0.533
25	1.59	1.51	5.0	14.29	12.95	9.3	0.695

Before PECF **After PECF**

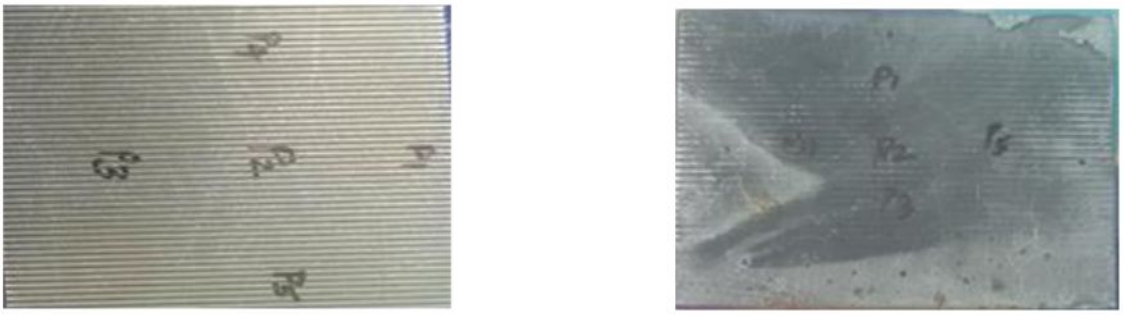

(a) **(b)**

Fig. 4.2: (a) surface of sample before experiment and (b) surface of sample after experiment**.**

From the above Table 4.2, where the experiment has been performed on a single sample which was time dependent study starting from 5 minutes to 25 minutes. This showed that the percentage change in arithmetical average roughness *'Ra'* (µm) increased to 64.5% at 20 minutes but not at 25 minutes where it was 5% and percentage change in average maximum height *'Ry'* (µm) increased to 50.2% at 20 minutes and 9.3% at 25%. The achieved minimum surface roughness of 12.95 (µm) was found at 25 minutes finishing duration and 14.29 at 20 minutes time with material removal rate at 0.695 (mm^3/s) at 25 minutes and 0.553 (mm^3/s) at 20 minutes. The image of the sample is shown in Fig 4.2(a) and Fig 4.2(b).

Table 4.3: Results for Sample 3 of pilot stage first experiment

Finishing duration (min)	Arithmetical Average Roughness *'Ra'* (µm)			Average Maximum Height *'Ry'* (µm)			MRR (mm^3/s)
	Before PECF	After PECF	'%' change	Before PECF	After PECF	'%' change	
5	5.96	5.59	6.2	52.83	45.65	13.5	0.183
10	5.59	4.26	23.7	45.65	28.7	37.1	0.325
15	4.26	1.874	56	28.7	15.007	47.7	0.533
20	1.874	1.633	12.8	15.007	12.627	15.8	0.658
25	1.633	1.244	23.8	12.627	11.396	9.7	0.800

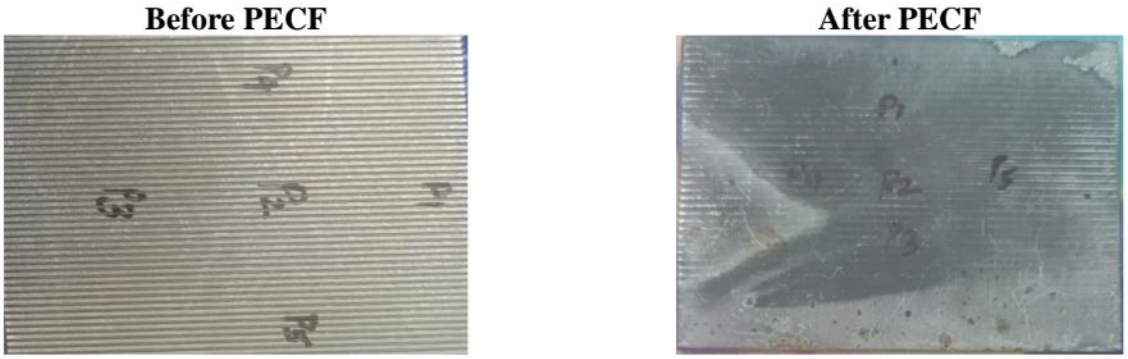

Fig. 4.3: (a) surface of sample before experiment (b) surface of sample after experiment

Discussion

From the above Table 4.3, where the experiment has been performed on a single sample which was time dependent study starting from 5 minutes to 25 minutes. This showed that the percentage change in arithmetical average roughness *'Ra'* (µm) increased to 23.8% at 25 minutes and at 25 minutes where it was 12.8% and percentage change in average maximum height *'Ry'* (µm) increased to 9.7% at 25 minutes and 15.8% at 20 minutes. The achieved minimum surface roughness of 11.396 (µm) was found at 25 minutes finishing duration and 12.627 at 20 minutes time with material removal rate at 0.800 (mm^3/s) at 25 minutes and 0.658 (mm^3/s) at 20 minutes. The image of the sample is shown in Fig 4.3(a) and Fig 4.3(b).

Table 4.4: Results for Sample 4 of pilot stage first experiment

Finishing duration (min)	Arithmetical Average Roughness *'Ra'* (µm)			Average Maximum Height *'Ry'* (µm)			MRR (mm^3/s)
	Before PECF	After PECF	'%' change	Before PECF	After PECF	'%' change	
5	5.90	5.23	11.3	44.80	34.52	22.9	0.429
10	5.23	4.02	23.1	34.52	29.80	13.6	0.745
15	4.02	3.81	5.2	29.80	25.12	15.7	0.404
20	3.81	2.21	41.9	25.12	18.73	25.4	0.310
25	2.21	1.79	19	18.73	12.95	30.8	0.695

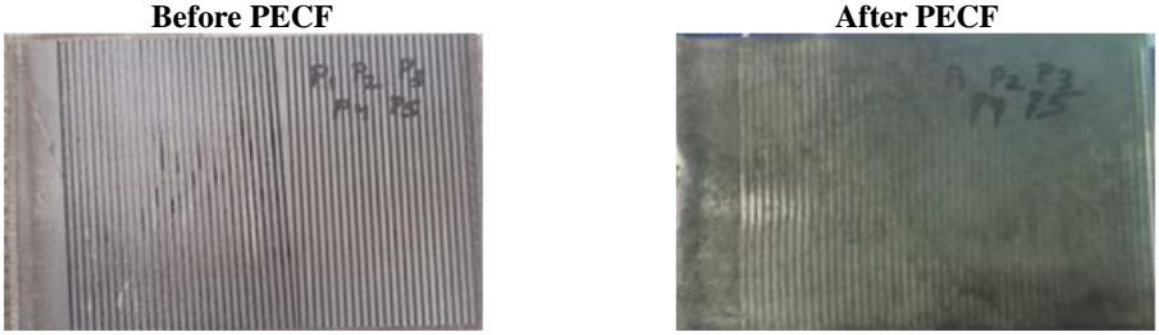

Fig. 4.4: (a) surface of sample before experiment (b) surface of sample after experiment.

Discussion:

From the above Table 4.4, where the experiment has been performed on a single sample which was time dependent study starting from 5 minutes to 25 minutes. This showed that the percentage change in arithmetical average roughness *'Ra'* (µm) increased to 19% at 25 minutes and at 20 minutes where it was 41.9% and percentage change in average maximum height *'Ry'* (µm) increased to 30.8% at 25 minutes and 25.4% at 20 minutes. The achieved minimum surface roughness of 12.95 (µm) was found at 25 minutes finishing duration and 18.73 at 20 minutes time with material removal rate at 0.695(mm^3/s) at 25 minutes and 0.310 (mm^3/s) at 20 minutes. The image of the sample is shown in Fig 4.4(a) and Fig.4.4(b).

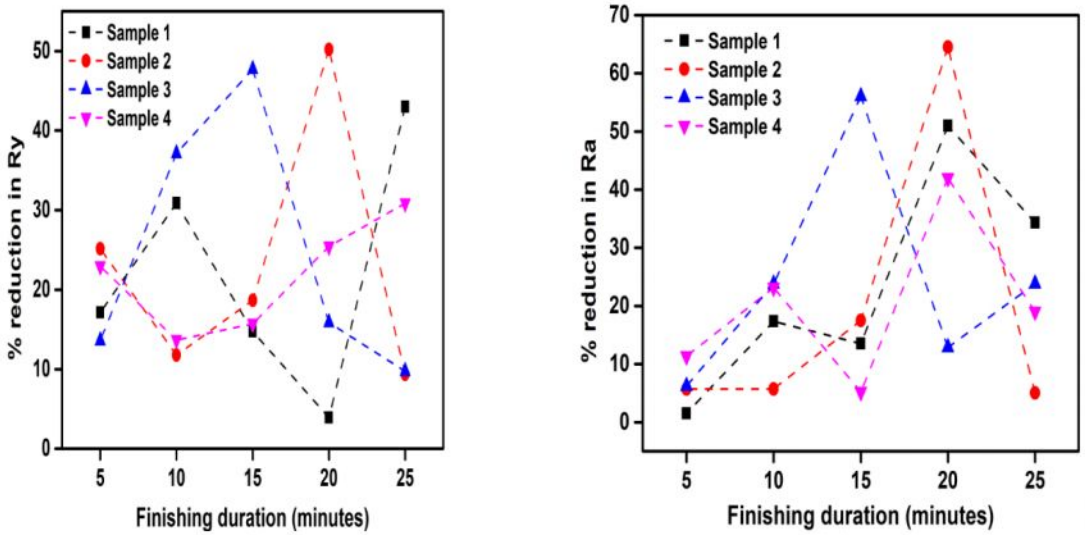

Fig. 4.5: (a) finishing duration with respect to % reduction in 'Ra' (b) finishing duration with respect to % reduction in 'Ry'.

The above graph in Fig. 4.5 (a) and (b) shows the percentage reduction in R_y with respect to the finishing duration of the PECF process and similarly, the graph (2) shows the percentage reduction in R_a with respect to the finishing duration at 5, 10, 15, 20 and 25 minutes. The experiments here were performed on four SS316L samples. As from the observations, the maximum finishing duration where the minimum surface roughness and maximum percentage reduction is varying in the range duration of between 15-25 minutes, but the common and optimum finishing duration value was achieved at 20 minutes where it denotes the peak in the form of red bubble. The Identified finishing duration in range of 15-25 minutes where the selected value was 20 minutes.

Observation drawn from the pilot stage 1 experiment:

In pilot stage-1 experiment of determination of finishing duration, the minimum surface roughness identified is within the range of 15 to 25 minutes. In this time dependent study, The changes (reduction) in surface roughness is due to varying & constant parameters at different levels. With non-uniform Inter-electrode gap and at certain flow of current, the workpiece material begins getting deteriorated. (Liu et al., 2022)At 20 minutes of finishing duration, more samples are attaining percentage reduction in 'Ra' and similarly percentage reduction for *'Ry'*.

4.2 Result of second stage of pilot experiment and observations

Identified optimum values of Flow Rate and Composition of Electrolyte

Table 4.5: Result showing second stage of pilot experiment

Exp. No.	Flow Rate (l/min)	Composition (%)		Arithmetical Average Roughness *'Ra'* (µm)			Average Maximum Height *'Ry'* (µm)			MRR (mm^3/s)
		NaCl	$NaNO_3$	Before PECF	After PECF	'%' change	Before PECF	After PECF	'%' change	
1.	10	100	---	5.3	5.1	3.7	52.1	16.9	67.5	0.180
2.	15			3.3	3.23	2.1	48	14.66	69.4	0.31
3.	20			2.9	2.7	6.8	44.6	11.42	74.3	0.361
4.	10	75	25	2.3	1.8	21.7	48.12	11.33	76.4	0.265
5.	15			2.125	1.19	44	44.16	10.1	77.1	0.5275
6.	20			1.61	1.325	17.7	41.25	9.87	76	0.3675
7.	10	50	50	6.6	5.9	10.6	50.51	25.39	49.7	0.044
8.	15			5.82	5.39	7	44.16	10.1	77.1	0.1625
9.	20			5.1	4.01	21.3	45	19.22	57.2	0.174
10.	10	25	75	7.7	7.5	2.5	44.2	42.8	3.1	0.060
11.	15			7.34	7.12	2.9	43.9	41.0	6.6	0.078
12.	20			6.6	6.14	6.9	41.6	39.23	5.6	0.0525
13.	10	---	100	7.2	7.071	1.7	48.24	46.31	4	0.015
14.	15			7.51	7.132	5	46.5	45.2	2.7	0.028
15.	20			6.94	6.812	1.8	46.1	41.26	10.4	0.064

Fig. 4.6: (a) surface of sample before experiment and (b) surface of sample after experiment.

Discussion: In this stage of experiment, from the table 4.5 we can observe that 15 experiments were conducted in 5 samples by using 3 varying levels of electrolyte flow rate that was 10 liter/min, 15 liter/min and 20 liter/min with 5 varying levels of composition of the electrolyte that was at 100% NaCl, 75% NaCl + 25% $NaNO_3$, 50% NaCl + 50% $NaNO_3$, 25% NaCl +75% $NaNO_3$, 100% $NaNO_3$. At 75% NaCl + 25% $NaNO_3$ composition and

15liter/min flow rate, maximum percentage reduction in (R_a) was achieved as 21.7% and at 10liter/min it was 10.6%. Similarly, in case of average maximum height (R_y) maximum percentage reduction was achieved was 77.1% and minimum surface roughness attained was 9.87(μm). The image of the sample is shown in Fig. 4.6 (a) and (b). The maximum flow rate that is above 10 liter/min was somewhat challenging to control due to safety measures and it caused some wear from the surface of the workpiece. At other levels of composition of the electrolyte such as 100% $NaNO_3$ it showed no such changes in material removing as it forms a protective passivation layer or film on the surface of the workpiece which stops the electrolytic dissolution to occur efficiently and lessens the ability to remove the material. However, $NaNO_3$ prevents the corrosion rate from the material.

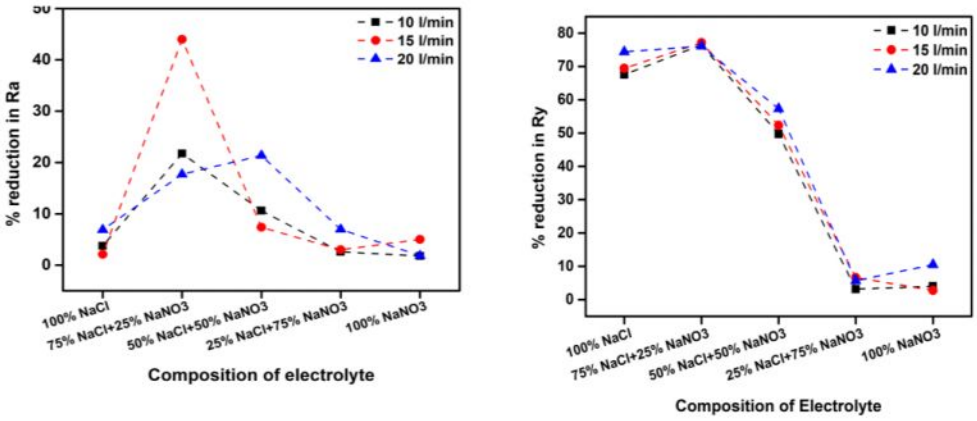

(b)

Fig. 4.7: (a) Composition and flow rate of electrolyte with respect to % reduction in Ra (b) Composition and flow rate of electrolyte with respect to % reduction in Ry.

The above graph in Fig. 4.7 (a) shows the percentage reduction in R_y with respect to the composition and flow rate of the electrolyte of the ECF process and similarly, the graph in Fig. 4.7 (b) shows the percentage reduction in R_a . The experiments here were performed on five SS316L samples. As from the observations, the minimum surface roughness and maximum percentage reduction is varying at few parametric levels of the flow that was at 10 liter/min, 15liter/min and 20 liter/min but optimum values of flow rate and composition of the electrolyte was achieved at 10 liter/min flow rate and 75% NaCl + 25% $NaNO_3$ where it denotes the peak in the form of red bubble and moderate level of flow rate of electrolyte in the form of black square. Identified flow rate and composition of electrolyte: 10 litre/min and 75% NaCl + 25% $NaNO_3$

Observation drawn from the pilot stage 2 experiment:

From the pilot stage 2 experiment determination of flow rate and composition of electrolyte:

The flow rate and composition of the electrolyte at which the surface roughness reached to a minimal level has been found at 10 litre/minute and 75% NaCl + 25% $NaNO_3$.There has been no

such change observed in percentage reduction of 'Ra' and 'Ry' where more composition of $NaNO_3$ electrolyte is used. More composition of electrolyte NaCl is found to have high material removal rate. The optimal parameters of flow rate and composition of electrolyte helped in maintaining surface uniformity and preventing thermal damage to the workpiece and achieving desired results.(Barril et al., 2002)The optimal composition of the electrolyte helped in preferential removal of certain phases and impurities which led controlled and uniform surface finish.

4.3 Result of Main Experiment: To identify Optimum Values of Voltage, Pulse-on Time, Pulse-off Time. Electrolyte Concentration

Table 4.6 : Result showing the responses for main experiment

Exp. No.	Varying Parameters				Arithmetical Average Roughness *'Ra'* (µm)			Average Maximum Height *'Ry'* (µm)			MRR (mm^3/s)
	Voltage (V)	Concentration (C)	Pulse on time (t_{on})	Pulse off time (t_{off})	Before PECF	After PECF	'%' change	Before PECF	After PECF	'%' change	
1.	25	5	3	4	5.312	4.022	24	42.1	28.6	32.0	0.093
2.	20	5	2	2	5.11	4.25	16.8	44.66	23.55	47.2	0.096
3.	25	5	3	2	4.36	3.19	26.8	49.20	23.4	52.4	0.090
4.	25	5	2	6	6.10	4.05	33.6	39.66	19.92	49.7	0.077
5.	30	5	2	4	6.218	4.105	33.9	35.43	20.17	43.0	0.077
6.	25	5	2	6	3.9	2.2	43.5	35.22	19.10	45.7	0.045
7.	20	5	2	4	4.72	3.88	17.7	37.45	17.34	53.6	0.043
8.	30	5	3	6	4.38	3.03	30.8	38.190	20.011	47.6	0.043
9.	20	5	3	6	5.59	4.16	25.5	38.21	19.26	49.5	0.042
10.	25	5	4	2	3.525	2.067	41.3	41.16	24.22	41.1	0.045
11.	20	5	4	6	6.4	5.2	18.75	40.05	18.37	54.1	0.060
12.	30	5	2	2	4.99	3.60	27.8	34.82	16.59	52.3	0.053
13.	30	5	4	6	3.78	2.01	46.8	33.219	16.25	51.0	0.054
14.	25	5	4	4	4.62	3.13	31.8	31.70	17.60	44.4	0.060
15.	25	5	2	6	3.64	2.44	32.9	35.8	18.1	49.4	0.060
16.	20	10	6	2	3.181	1.910	39.9	36.74	15.26	58.4	0.043
17.	30	10	2	6	6.052	3.445	43.8	42.7	16.8	60.6	0.050
18.	25	10	2	6	6.1	3.9	36.0	42.289	15.117	64.2	0.042
19.	25	10	4	6	3.669	2.118	42.2	36.1	14.3	60.3	0.057
20.	25	10	3	6	4.183	2.644	36.7	44.29	15.23	65.6	0.056
21.	25	10	2	2	5.16	2.98	42.2	39.28	14.86	62.1	0.051
22.	25	15	2	4	7.14	3.33	53.3	40.16	13.10	67.3	0.037
23.	30	15	2	6	5.75	2.81	51.1	44.29	16.18	63.4	0.056
24.	25	15	2	2	6.482	3.601	44.4	46.38	15.39	66.8	0.047
25.	20	15	2	6	5.65	3.02	46.5	35.24	11.66	66.9	0.043
26.	25	15	4	6	4.226	2.067	51.0	34.71	11.25	67.5	0.082
27.	25	15	3	6	5.179	2.112	59.2	36.82	10.46	71.5	0.120

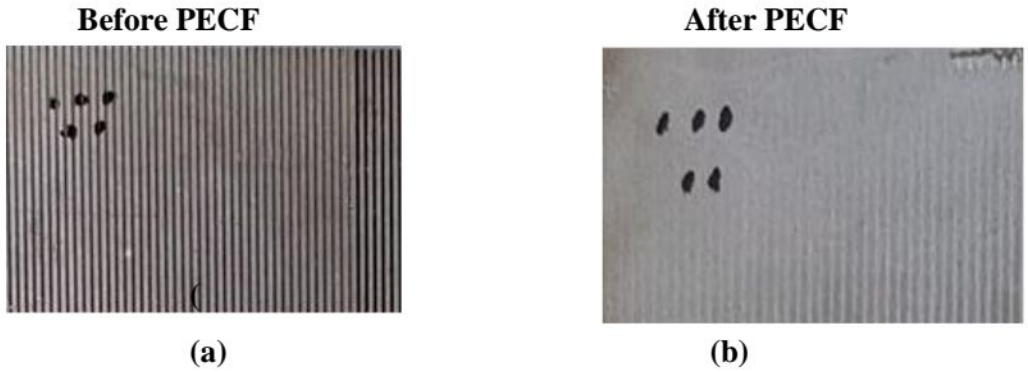

Fig. 4.8: (a) surface of sample before experiment (b) surface of sample after experiment

The figure 4.9 (a), 4.9 (b) and 4.9 (c) is showing the effect of voltage in the main experiment with percentage reduction in R_a and R_y with respect to different parameters such as with pulse on time, pulse off time and with concentration. Similarly, in fig 4.10 (a) and fig 4.10 (b) it is showing the percentage reduction in effect of electrolyte concentration with pulse off time and pulse on time. Also, in fig. 4.11 the graph shows the percentage reduction with respect to pulse on time and pulse off time.

Result of Main Experiment: Effect of Voltage

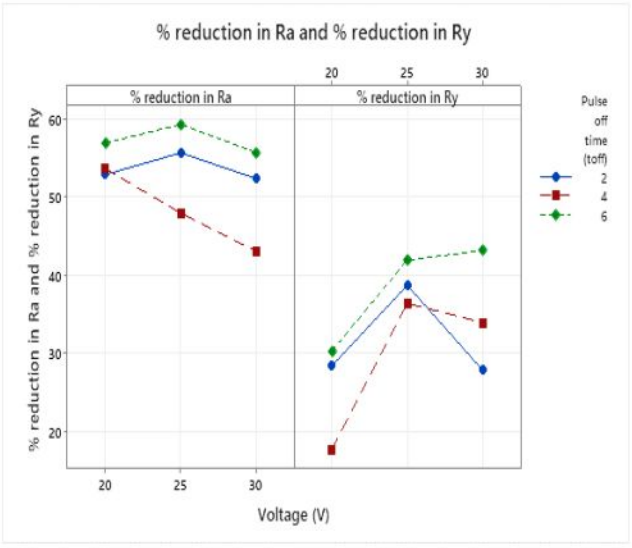

(a)

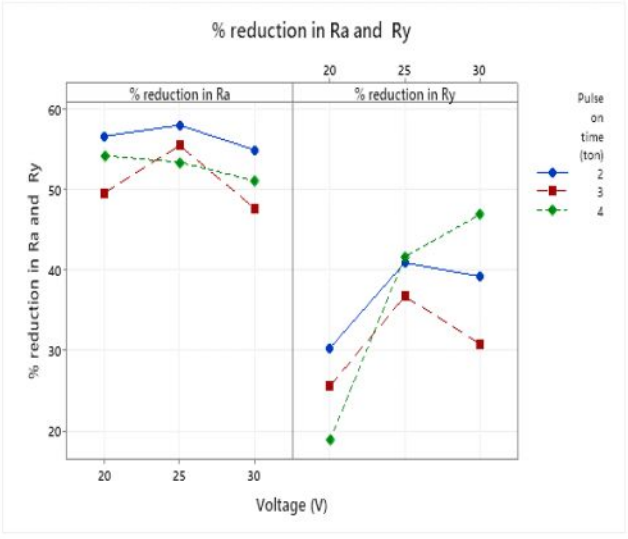

(b)

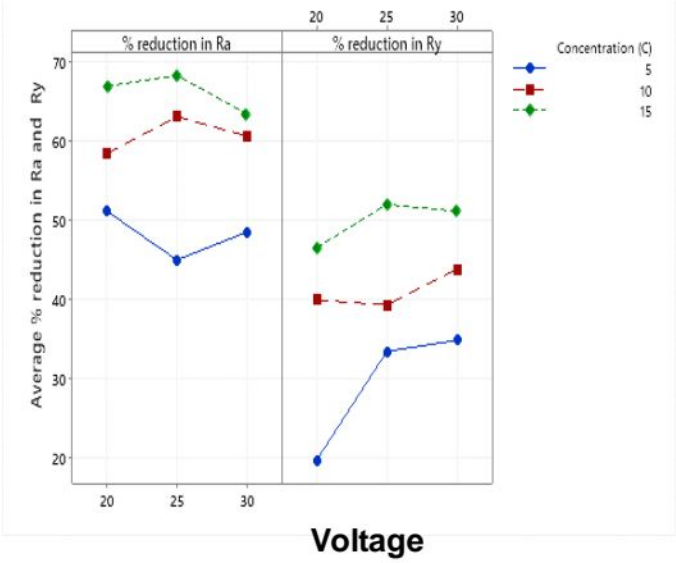

(c)

Fig.4.9: % reduction in R_a and R_y showing with respect to (a) effect of voltage with pulse off time (b) effect of voltage with pulse on time (c) effect of voltage with concentration.

Effect of Electrolyte Concentration

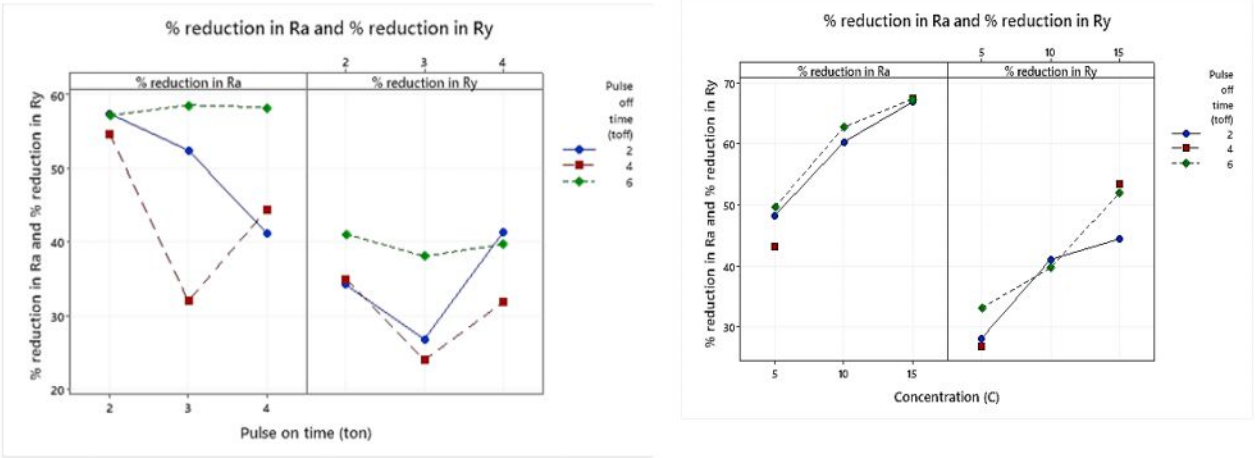

(a) **(b)**

Fig.4.10: % reduction in R_a and R_y showing with respect to (a) effect of pulse on time with pulse off time (b) effect of concentration with pulse off time

Effect on Pulse on time and pulse off time

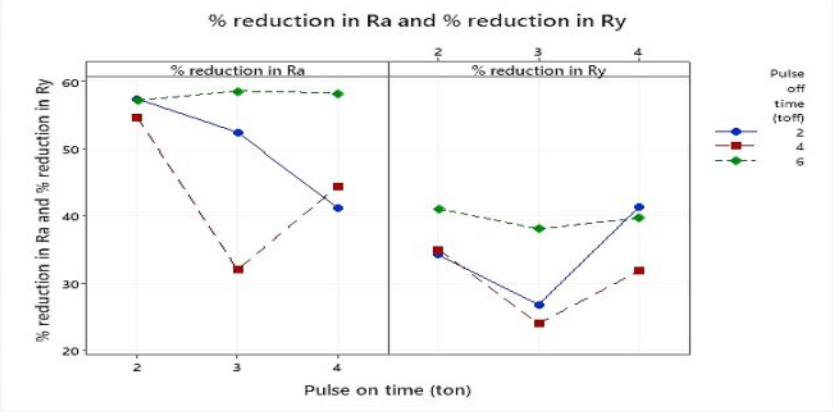

Fig.4.11: % reduction in R_a and R_y showing with respect to (a) effect of pulse on time with pulse off time.

Quadratic Equation for the Measured Responses

Equation for % reduction in R_a: Equation 4.1

$$R_a = -41 - 0.33V + 4.34C - 15.1 - 15.1T_{on} + 23.5T_{off} - 0.004V^2 - 0.161C^2 - 1.17T_{on}^2 - 0.225T_{off}^2 + 0.058V*C + 1.361V*T_{on} + -0.444\ V*T_{off} + 0.546C*T_{on} - 0.355\ C*T_{off} - 2.83\ T_{on} * T_{off}$$

Equation for % reduction in R_y: Equation 4.2

$$R_y = 136.6 - 8.94V + 5.76C - 22.3\ T_{on} + 11.1T_{off} + 0.156V^2 - 0.370\ C2 + 0.44\ T_{on}2 + 0.318\ T_{off}2 + 0.164\ V*C\ 0.738\ V*T_{on} - 0.449\ V*T_{off} + 0.273\ C*T_{on} - 0.303\ C*T_{off} - 0.16\ T_{on} * T_{off}$$

Equation for MRR: Equation 4.3

$$\textbf{MRR (mm}^3\textbf{/s)} = -0.363 + 0.0264V + 0.0030C + 0.2076ton - 0.0686T_{off} - 0.000451V^2 + 0.000198C^2 - 0.01820T_{on}^2 - 0.0029T_{off}^2 - 0.000682V*C$$

Discussion and observation drawn from the main experiment:

From the above Table 4.6 of main experiment where the four parameters: Voltage(V), Concentration(C), Pulse on time, T_{on}(ms) and Pulse off time, T_{off}(ms) are varying which needs to be optimized. Hence the values taken were at three levels. For voltage, it was 20V, 25V and 30V. For concentration, it was 5%, 10% and 15%. Similarly, for T_{on} and T_{off} it

2ms, 3ms, 4ms and 6ms. The maximum percentage reduction in case of arithmetical average roughness (R_a) was found at mainly three parametric levels such as for 25V, 15% conc., 2ms and 4ms it was 53.3%. Also, for 25V, 15% conc., 4ms and 6ms it was 51.0% and for 25V, 15% conc., 3ms and 6ms it was 59.2%. Similarly, in case of average maximum height (Ry) at same parametric levels it was found to be 67.3%, 67.5% and 71.5% with MRR as 0.037 mm^3/s 0.082 mm^3/s and 0.120 mm^3/s respectively. The image of sample is shown in figure 4.8 (a) and (b). Hence, we can see that the maximum percentage change in case of both R_a and Ry was found maximum at 25V, 15% conc., 3ms, 6ms. A low level of concentration of below 15% and voltage of below 20% showed slow material removal rate with no such big changes on the peaks and valleys of the surface. Thus, these optimum values of 25V, 15% conc., 3ms, 6ms has been carried out for the final confirmation experiment and increased susceptibility to surface erosion. Also, from the graphs shown in Fig. 4.9 (a) and Fig. 4.9 (b) it can be observed that the % change in R_a with respect to voltage and conc. and T_{on} , T_{off} is decreasing with increasing V, conc, T_{on} , T_{off} that is at 25V, 15% conc, and 3ms, 6ms pulse on and pulse off time. Similarly, from the graphs shown in Fig. 4.10 (a) and 4.10 (b) the % change in R_y with respect to voltage and conc. and T_{on}, T_{off} is also decreasing with increasing V, conc, T_{on} , T_{off} that is at 25V, 15% conc, and 3ms, 6ms pulse on and pulse off time. Hence, the optimal values concluded from the parameters are 25V, 15% conc., T_{on} 3ms and T_{off} 6ms.

4.4 Result of Confirmation Experiment

Surface finish of µ-PAM Manufactured Tibial Tray using identified optimum values of T_f, F, C, V, T_{on}, T_{off} and Conc.

Table 4.7: Result showing optimized values in confirmation experiment

Exp. No.	Optimum Parameters				Arithmetical Average Roughness *'Ra'* (µm)			Average Maximum Height *'Ry'* (µm)			MRR (mm^3/s)
	Voltage (V)	Concentration (C)	Pulse on time (t_{on})	Pulse off time (t_{off})	Before PECF	After PECF	'%' change	Before PECF	After PECF	'%' change	
1.(Tibial)	25	15	4	6	3.718	1.522	59.0	34.71	10.71	68.7	0.112
2.	25	15	4	6	5.39	2.65	50.8	36.71	11.24	69.3	0.072
3.	25	15	4	6	3.84	1.98	48.4	38.43	11.53	69.9	0.061
4.	25	15	4	6	3.116	1.237	60.3	40.05	12.69	68.3	0.055

Discussion and observation drawn from the confirmation experiment:

From the Table 4.7 optimum values of the parameters that are V, Conc, T_{on} and T_{off}, the derived values: Voltage:25V, Concentration:15%, T_{on}:3ms and T_{off}:6ms, a good surface

roughness was observed.The total percentage reduction in (R_a) was found to be 59.0%(tibial), 50.8%(sample 2), 48.4%(sample 3) and 60.3%(sample 4) and same in Ry it is 68.7%(tibial), 60.06%(sample 2), 69.9% (sample 3)and 68.3%(sample 4) with MRR be 0.091 mm^3/s(tibial), 0.072 mm^3/s(sample 2), 0.061%(sample 3) and 0.055%(sample 4). Also, the Arithmetical average roughness (R_a) reduced from 3.178 µm to 1.522 µm(tibial), 5.39 µm to 2.65 µm(sample 2), 3.84 µm to 1.98 µm(sample 3) and 3.116 µm to 1.237 µm(sample 4). Similarly, Average maximum height (R_y) reduced from 34.71 µm to 10.71 µm(tibial), 36.71 µm to 14.66 µm(sample 2), 38.43 µm to 11.53(sample 3) µm and 40.05 µm to 12.69 µm(sample 4). The optimal values of pulse off and pulse on time reduced the temperature rise and prevented the heating of the workpiece which gave better material removal rate. At other parametric values, no such satisfactory change was observed on the surface of component.

4.5 Effect of the different parameters:

Depending on the required metal being electrofinished, the desired result, and the tools being used, these characteristics can have different effects. To get the intended outcomes, choosing the best parameters frequently calls for experimentation. These specified input parameter ranges can be supported by the talks that follow:

- **Effect of applied voltage:** From the table it is evident that maximum values of average percentage improvements across all parameters increases as the amount of applied voltage rises to 25 volts, while the highest values of the surface roughness characteristics are reached at lower voltage levels (i.e., 10,15 and 20 volts) and similarly the material surface characteristics deteriorates at 30 volts. Additionally, 25 volts as the applied voltage values results in the simultaneous improvement in the parameters of responses in both main and confirmation experiment. This is because the material removal rate is low at lower applied voltage levels,(et al., 2019) which reduces surface roughness by minimizing high peaks, whereas the substance eliminated at a lower voltage was insufficient to produce significant alterations. At higher values of applied voltage, the higher material removal rate was observed which leads to non-uniform removal of material from the surface of the workpiece and thus deteriorates the surface finish. Therefore, To simultaneously improve all the surface roughness taken into consideration, a moderate applied voltage of 25 volts is determined to be the best value.
- **Effect of pulse-on time and pulse-off time:** With longer pulse-on times in PECF, more time is allowed for the finishing action to take place, which results in an increase in material removal rate. The purpose of the pulse-off period is to remove all reaction products and keep the IEG clean for the subsequent pulse-on period. Therefore, a smaller

value of pulse-on time will allow very little duration for the finishing and result in a lower MRR that may cure imperfections like surface roughness. The optimal value for achieving simultaneous improvement in the surface roughness characteristics studied was a longer pulse-on time, or 6 ms Lower values of pulse-off time, i.e., 3 ms were chosen as its optimum value because they offer the finishing action enough time to complete the finishing process and allow for the removal of the produced sludge products to occur more quickly.

- **Effect of finishing time:** More finishing cycles are used when the finishing duration is longer, which helps to increase the material removal rate. A balance between surface, material removal rate and process stability are required for high MRR in PECF which helps in achieving improved surface quality and precision. (Shaikh and Jain, 2015) As a result, 20 minutes was chosen in the time dependent study as the ideal finishing time to accomplish simultaneous improvements in the surface roughness characteristics under consideration.
- **Effect of electrolyte concentration:** During pulsed electrochemical finishing, the concentration of the electrolyte influences the current density. In general, larger electrolyte concentrations lead to an increase in current density, which can speed up the rate of material removal.(Kumar et al., 2023) Lower electrolyte concentrations may produce surfaces that are smoother and have less surface roughness. Due mostly to higher current densities and higher dissolving rates, higher concentrations can result in an increase in surface roughness. Hence, as a result 15% concentration of electrolyte was chosen.
- **Effect of flow rate of electrolyte:** Typically, MRR increases with higher flow rates. Increased flow rates maintains steady flow of fresh electrolyte and enhance cooling by preventing excessive heat buildup.(Taylor and Inman, 2014) Optimal flow rate of 10litre/minute is chosen which encourage consistent material removal and reduce regional impacts like overcutting or pitting.
- **Effect of composition of the electrolyte:** With modified composition,material removal rate can be regulated. Surface integrity might vary depending on the electrolyte content.It may influence wear of the workpiece and reduced dimensional accuracy. Process efficiency can be increased, cycle times can be shortened, and energy usage can be decreased by optimising the electrolyte composition. Thus, by keeping in considerations all such factors an optimal composition of 75% NaCl and 25% $NaNO_3$ was chosen as an electrolyte.

- **Effect of Interelectrode gap (*IEG*):** Smaller *IEG* typically result in surfaces that are smoother and have lower roughness ratings. Because of the concentrated current in that area and the increased current density close to the narrower gap, the material is removed more carefully, resulting in finer and smoother surface. Larger gaps decrease the current density and allow lower material removal.(Zhou et al., 2019) Hence, by varying the different values of *IEG* parameter at 0.75mm, 1mm, 1.5mm. The optimal value deduced to be at 1mm.

4.6 Analysis of the Tibial Component and Confirmation Samples

The average maximum height (R_y) of tibial reduces to 10.71 µm.Initially, it was 34.25 µm with a percentage reduction at 68.7%. Similarly, the arithmetical average roughness (R_a) reduces to 1.522 µm. Initially, it was 3.718 µm with a percentage reduction at 59.0%.

Before PECF **After PECF**

(a) **(b)**

Fig.4.12: (a) surface of the tibial before PECF and (b) surface of the tibial after PECF

The two different phases of tibial tray are shown in figure 4.12 where Fig.4.12 (a) depicts the surface of tibial before the PECF experiment and Fig.4.12 (b) depicts the surface of the tibial after the PECF experiment.

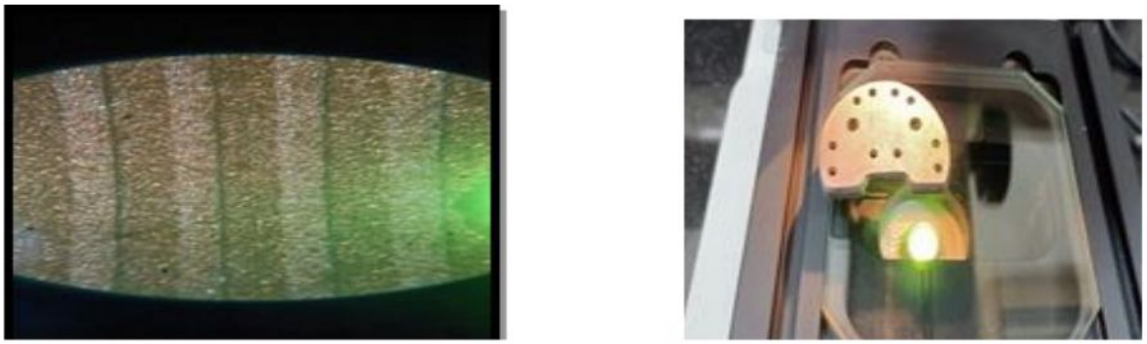

(a) **(b)**

Fig. 4.13: (a) Magnified image of grooves (b) measurement of grooves by tool makers microscope.

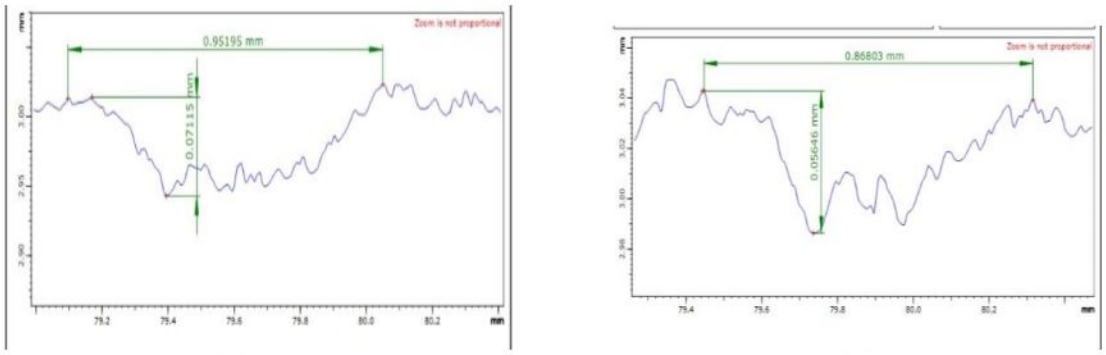

(a) **(b)**

Fig. 4.14: (a) graph showing width and depth of grooves (b) graph showing width and depth of grooves measured by Mahr surf LD 130.

Groove dimensions including width and depth has been measured by tool makers microscope. It visually inspected the profile of groove with high precision measurements, analysis capabilities for grooves. It detected no defects within the groove such as cracks, scratches and irregularities. It measured the depth as 0.071 mm, 0.056 mm and width as 0.951 mm, 0.868 mm respectively. The magnified image of grooves taken from the tool makers microscope is shown in the above figure 4.13 (a) and 4.13 (b). Also, the measurement of those grooves with its width and depth is shown in the figure 4.14 (a) and 4.14 (b). The 3D surface plot of roughness providing topography and showing the texture of the surface with different peaks and valleys is depicted in Fig. 4.15 (a) and Fig. 4.15 (b) and the roughness profile graph of the finished tibial surface is depicted in the Fig. 4.14 (b).

3D SURFACE TOPOGRAPHY OF SS 316L BEFORE PECF

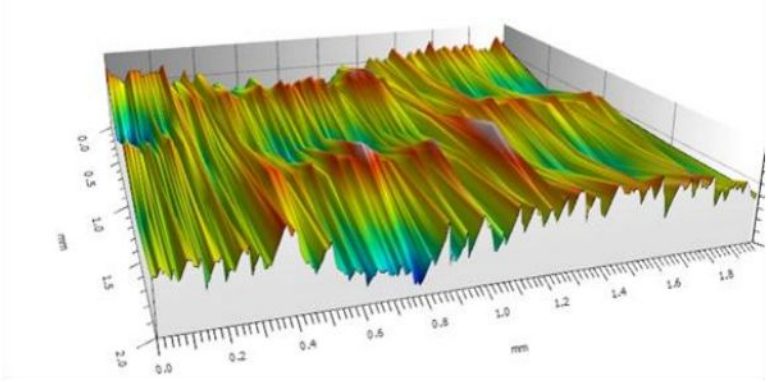

(a)

3D SURFACE TOPOGRAPHY OF SS 316L AFTER PECF

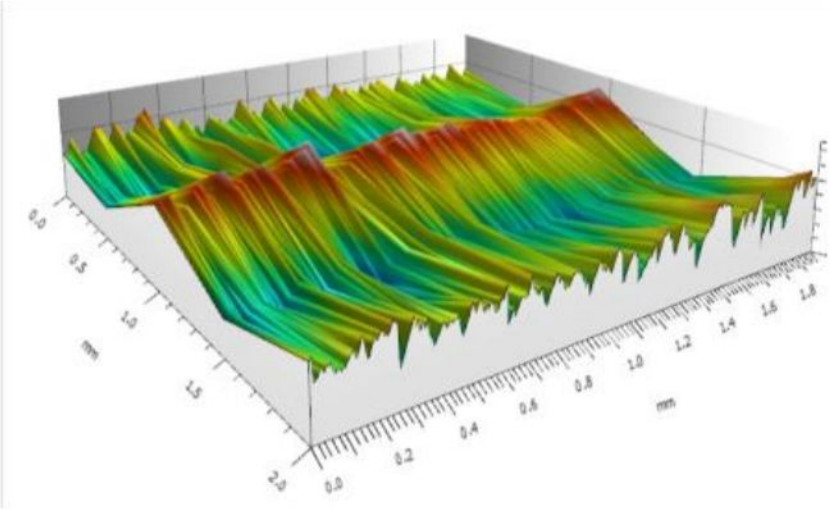

(b)

Fig.4.15: (a) 3D surface topography of unfinished tibial surface b) 3D surface topography of finished tibial surface: using the identified optimum values of pulse-on time, pulse-off time, finishing time and voltage.

The microscopic image of surface of the tibial showing the grooves patches depicting a rough surface in Fig. 4.16 (a) and Fig.4.16 (b) is showing a smooth surface with no such oxide layers or formation of contamination and no wear. These results are deduced after getting the optimal values by varying different parameters at different levels.

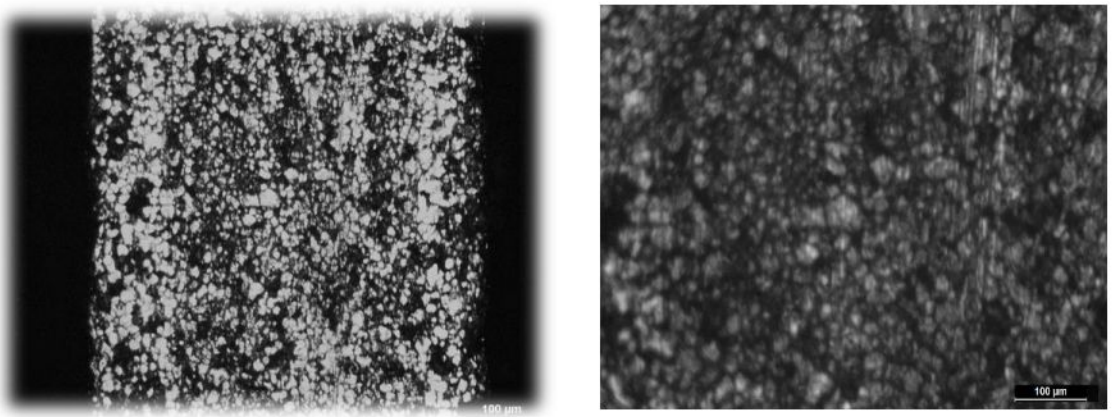

(a) **(b)**

Fig.4.16: (a) optical microscopic image of unfinished surface of tibial (b) optical microscopic image of finished surface of tibial taken from optical microscope

In the figure 4.17, the images is showing the roughness graph of the tibial tray SS316L of before and after the PECF process. In the first graph, fig:4.17(a) it is showing the maximum roughness at peak and hence in fig:4.17(b) it is showing reduction in roughness

Surface Roughness Plot of SS 316L Tibial Tray Before PECF

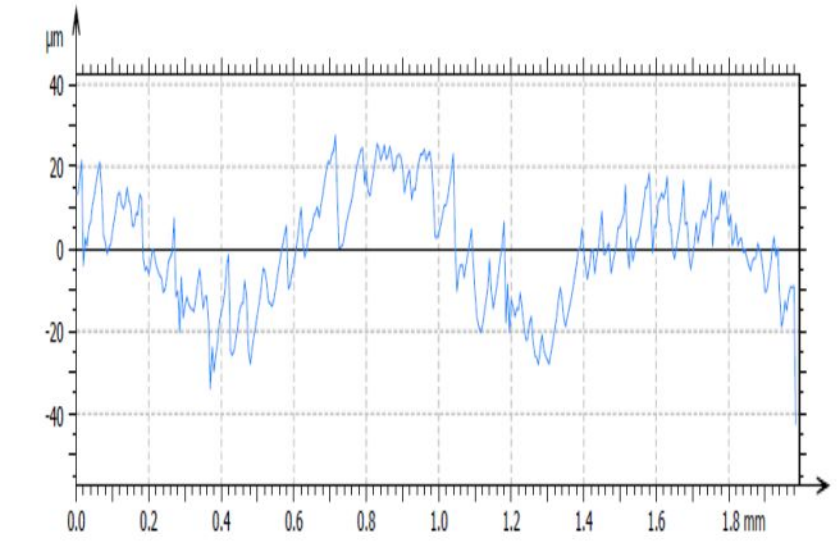

(a)

Surface Roughness Plot of SS 316L Tibial Tray After PECF

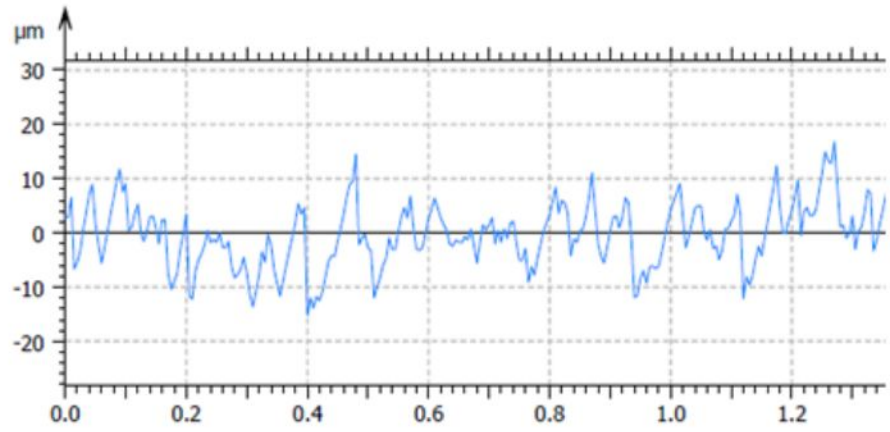

(b)

Fig.4.17: (a) Roughness profile of tibial tray before PECF (b) Roughness profile of tibial tray after PECF

Confirmation Sample: The average maximum height (R_y) of confirmation sample reduces to 14.66 µm.Initially, it was 50.8 µm with a percentage reduction at 60.06%. Similarly, the arithmetical average roughness (R_a) reduces to 2.65 µm. Initially, it was 5.39 µm with a percentage reduction at 50.8%.The two different phases of confirmation sample is shown in the below figure 4.14 where fig.4.18 (a) is depicting the surface of confirmation sample before the PECF experiment and Fig. 4.18 (b) is depicting the surface of the confirmation sample after the PECF experiment.

Before PECF **After PECF**

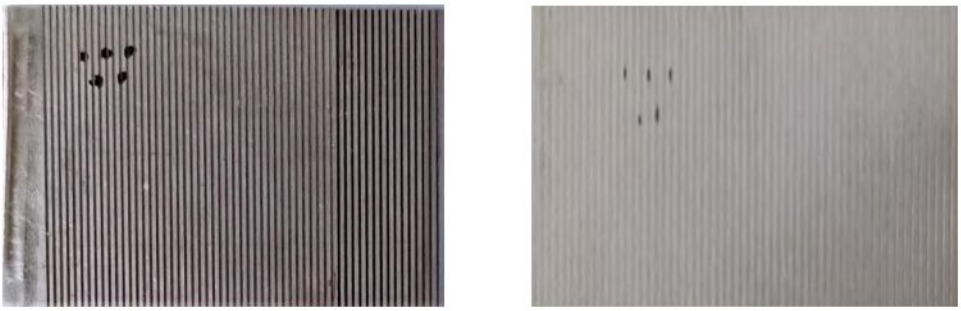

(a) **(b)**

Fig. 4.18: (a) surface of sample before experiment (b) surface of sample after experiment

The microscopic image of surface of the confirmation sample showing the grooves patches depicting a rough surface in Fig.4.19 (a) and figure 4.19 (b) is showing a smooth surface with no such oxide layers or formation of contamination and no wear. These results are deduced after getting the optimal values by varying different parameters at different levels.

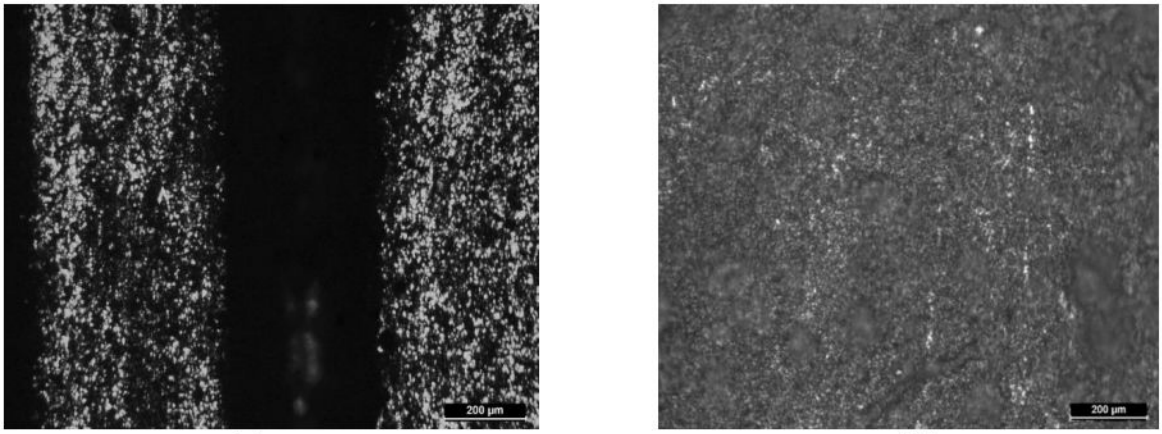

(a) **(b)**

Fig. 4.19: (a) optical microscopic image of unfinished surface of confirmation sample (b) optical microscopic image of finished surface of confirmation taken from optical microscope.

Chapter 5

Conclusion and Scope for the Future Work

This chapter summarises the results of the current investigation and offers suggestions for further research.

5.1 Conclusions

The following conclusions are drawn from research on **µ-PAM Manufactured Tibial Tray** surface quality that was completed by pulsed electrochemical finishing.

- Studied effects of finishing duration (t), electrolyte composition (E), electrolyte flow rate (F), electrolyte concentration (C), voltage (V), pulse-on time (T_{on}), pulse-off time (T_{off}) on % reduction in avg and max. surface roughness of SS 316L samples
- Identified their optimum values as 20 minutes; 75% NaCl and 25% $NaNo_3$; 10 lpm; 15%; 25 volt; 3 ms; and 6 ms respectively for finishing SLM manufactured Tibial Tray of SS 316L.
- The identified optimum values of T_{on}, T_{off}, V and C yielded values of PIR_a as 59% and PIR_y as 68.7%. Reduction in roughness parameters lead to longer service life.
- It also improved the overall surface of PECF finished component without any damage to its surface

.

5.2 Directions for the Future Research

- Obtaining the required level of accuracy and precision in fabrication of minituarized (micro and nano-scale metallic components) in areas such as electronics and biomedicine for micro/nano manufacturing.
- Further exploration and optimization of sustainability of PECF process to reduce its effects on the environment.
- Advancement of automated PECF integrating artificial intelligence and use of robotic arm may make it possible to finish complex components effectively without the assistance of human being.

Appendix: Specifications of the Measuring Instruments

- **3D Surface Roughness cum Contour Tracer (Gear Research LAB, IIT Indore)**

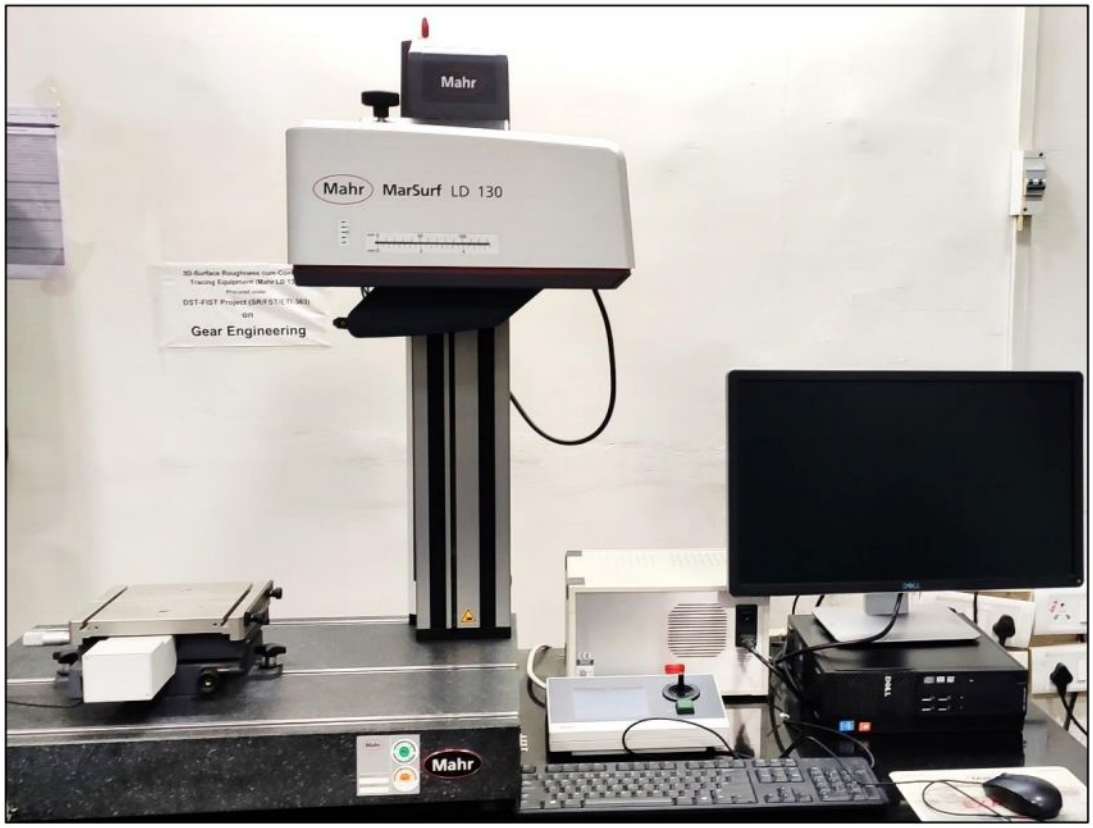

Make	Mahr GmbH
Model	MarSurf LD 130
Resolution	0.8 nm
Positioning speed	0.02 mm/s to 200 mm/s
Measuring speed	0.02 mm/s to 10 mm/s; for roughness measurements 0.1 mm/s to 0.5 mm/s is recommended
Measuring range (mm)	13 mm (100 mm probe arm) 26 mm (200 mm probe arm
Traversing lengths	0.1 mm - 130 mm
Measuring force (N)	0.5 mN to 30 mN, software-adjustable

- **Optical Microscope (Gear Research Lab, IIT Indore)**

Specification of Optical Microscope	
Model	Leica DM2500 M
Power supply	Stabilized universal power supply unit, 90–230 V for 12 V 30 W
Magnifying Range	10X, 100X
Software	Leica “QMW” for image analysis
Image Analysis	Digital
Attachment	Polarise

References

Barril, S., Debaud, N., Mischler, S., Landolt, D., 2002. A tribo-electrochemical apparatus for in vitro investigation of fretting-corrosion of metallic implant materials. Wear 252, 744–754. https://doi.org/10.1016/S0043-1648(02)00027-3

Bryant, M., 2019. FRETTING CORROSION CHARACTERISTICS OF TI6AL4V VERSUS TMZF Fretting corrosion characteristics of Ti6Al4V vs . TMZF titanium alloys in simulated body fluid.

Ishimoto, T., Ozasa, R., Nakano, K., Weinmann, M., Schnitter, C., Stenzel, M., Matsugaki, A., Nagase, T., Matsuzaka, T., Todai, M., Kim, H.S., Nakano, T., 2021. Development of TiNbTaZrMo bio-high entropy alloy (BioHEA) super-solid solution by selective laser melting, and its improved mechanical property and biocompatibility. Scr. Mater. 194. https://doi.org/10.1016/j.scriptamat.2020.113658

Khan*, I.A., Rani, M., Deb, R.K., Bundel, B.R., 2019. Effect on Material Removal Rate and Surface Finish in ECM Process When Machining Stainless Steel-316 with Cu Electrode. Int. J. Recent Technol. Eng. 8, 2933–2941. https://doi.org/10.35940/ijrte.d6817.118419

Kumar, P., Dixit, P., Chaudhary, B., Jain, N.K., 2023. Surface finishing of an additively manufactured part using electrochemical jet machining. Mater. Today Commun. 35, 105581. https://doi.org/10.1016/j.mtcomm.2023.105581

Liu, H., Ye, M., Ye, Z., Wang, L., Wang, G., Shen, X., Xu, P., Wang, C., 2022. High-quality surface smoothening of laser powder bed fusion additive manufacturing AlSi10Mg via intermittent electrochemical polishing. Surf. Coatings Technol. 443, 128608. https://doi.org/10.1016/j.surfcoat.2022.128608

Mohammad, A.E.K., Wang, D., 2016. Electrochemical mechanical polishing technology: recent developments and future research and industrial needs. Int. J. Adv. Manuf. Technol. 86, 1909–1924. https://doi.org/10.1007/s00170-015-8119-6

Ogawa, M., Wako, S., Kunieda, M., Nakagawa, T., 2020. Research on ECM Finishing Process using Wire Electrode. Procedia CIRP 95, 706–711. https://doi.org/10.1016/j.procir.2020.02.328

Pant, M., Pidge, P., Kumar, H., Nagdeve, L., Moona, G., 2021. Additive manufacturing: The significant role in biomedical and aerospace applications. Indian J. Eng. Mater. Sci. 28, 330–342. https://doi.org/10.56042/ijems.v28i4.42550

Peto, M., Ramírez-Cedillo, E., Hernández, A., Siller, H.R., 2019. Structural design optimization of knee replacement implants for Additive Manufacturing. Procedia Manuf. 34, 574–583. https://doi.org/10.1016/j.promfg.2019.06.222

Rotty, C., Mandroyan, A., Doche, M.-L., Monney, S., Hihn, J.-Y., Rouge, N., 2019. Electrochemical Superfinishing of Cast and ALM 316L Stainless Steels in Deep Eutectic Solvents: Surface Microroughness Evolution and Corrosion Resistance. J. Electrochem. Soc. 166, C468–C478. https://doi.org/10.1149/2.1211913jes

Shaikh, J.H., Jain, N.K., 2015. Effect of finishing time and electrolyte composition on geometric accuracy and surface finish of straight bevel gears in ECH process. CIRP J. Manuf. Sci. Technol. 8, 53–62. https://doi.org/10.1016/j.cirpj.2014.09.002

Taylor, E.J., Inman, M., 2014. Electrochemical surface finishing. Electrochem. Soc. Interface 23, 57–61. https://doi.org/10.1149/2.F05143if

Wu, T.F., Cheng, T.P., Tsai, W.T., 2001. Effect of electrolyte composition on the electrochemical potentiokinetic reactivation behavior of Alloy 600. J. Nucl. Mater. 295, 233–243. https://doi.org/10.1016/S0022-3115(01)00558-X

Zhou, Q., Sheikh, S., Ou, P., Chen, D., Hu, Q., Guo, S., 2019. Corrosion behavior of Hf0.5Nb0.5Ta0.5Ti1.5Zr refractory high-entropy in aqueous chloride solutions. Electrochem. commun. 98, 63–68. https://doi.org/10.1016/j.elecom.2018.11.009